





## REVIEW ARTICLE

# Quantitative magnetic resonance imaging towards clinical application in multiple sclerosis

 **Cristina Granziera**,<sup>1,2</sup> **Jens Wuerfel**,<sup>3,4</sup> **Frederik Barkhof**,<sup>5,6</sup> **Massimiliano Calabrese**,<sup>7</sup> **Nicola De Stefano**,<sup>8</sup> **Christian Enzinger**,<sup>9</sup> **Nikos Evangelou**,<sup>10</sup>  **Massimo Filippi**,<sup>11,12</sup> **Jeroen J.G. Geurts**,<sup>13</sup> **Daniel S. Reich**,<sup>14</sup>  **Maria A. Rocca**,<sup>11</sup> **Stefan Ropele**,<sup>15</sup> **Àlex Rovira**,<sup>16</sup> **Pascal Sati**,<sup>14,17</sup>  **Ahmed T. Toosy**,<sup>18</sup> **Hugo Vrenken**,<sup>5</sup> **Claudia A. M. Gandini Wheeler-Kingshott**<sup>18,19,20</sup> and **Ludwig Kappos**<sup>1,2</sup> on behalf of the **MAGNIMS Study Group**<sup>†</sup>

†Appendix 1.

Quantitative MRI provides biophysical measures of the microstructural integrity of the CNS, which can be compared across CNS regions, patients, and centres. In patients with multiple sclerosis, quantitative MRI techniques such as relaxometry, myelin imaging, magnetization transfer, diffusion MRI, quantitative susceptibility mapping, and perfusion MRI, complement conventional MRI techniques by providing insight into disease mechanisms. These include: (i) presence and extent of diffuse damage in CNS tissue outside lesions (normal-appearing tissue); (ii) heterogeneity of damage and repair in focal lesions; and (iii) specific damage to CNS tissue components. This review summarizes recent technical advances in quantitative MRI, existing pathological validation of quantitative MRI techniques, and emerging applications of quantitative MRI to patients with multiple sclerosis in both research and clinical settings. The current level of clinical maturity of each quantitative MRI technique, especially regarding its integration into clinical routine, is discussed. We aim to provide a better understanding of how quantitative MRI may help clinical practice by improving stratification of patients with multiple sclerosis, and assessment of disease progression, and evaluation of treatment response.

- 1 Neurologic Clinic and Policlinic, Departments of Medicine, Clinical Research and Biomedical Engineering, University Hospital Basel and University of Basel, Basel, Switzerland
- 2 Translational Imaging in Neurology (ThINk) Basel, Department of Biomedical Engineering, University Hospital Basel and University of Basel, Basel, Switzerland
- 3 Medical Image Analysis Center, Basel, Switzerland
- 4 Quantitative Biomedical Imaging Group (qbig), Department of Biomedical Engineering, University of Basel, Basel, Switzerland
- 5 Department of Radiology and Nuclear Medicine, Amsterdam Neuroscience, multiple sclerosis Center Amsterdam, Amsterdam University Medical Center, Amsterdam, The Netherlands
- 6 UCL Institutes of Healthcare Engineering and Neurology, London, UK
- 7 Neurology B, Department of Neurosciences, Biomedicine and Movement Sciences, University of Verona, Verona, Italy
- 8 Neurology, Department of Medicine, Surgery and Neuroscience, University of Siena, Italy
- 9 Department of Neurology and Division of Neuroradiology, Medical University of Graz, Graz, Austria
- 10 Division of Clinical Neuroscience, University of Nottingham, Nottingham, UK
- 11 Neuroimaging Research Unit, Institute of Experimental Neurology, Division of Neuroscience, and Neurology Unit, IRCCS San Raffaele Scientific Institute, Milan, Italy
- 12 Vita-Salute San Raffaele University, Milan, Italy
- 13 Department of Anatomy and Neurosciences, multiple sclerosis Center Amsterdam, Neuroscience Amsterdam, Amsterdam University Medical Centers, location VUmc, Amsterdam, The Netherlands

Received July 09, 2020. Revised October 25, 2020. Accepted November 16, 2020.

© The Author(s) (2021). Published by Oxford University Press on behalf of the Guarantors of Brain.

This is an Open Access article distributed under the terms of the Creative Commons Attribution Non-Commercial License (<http://creativecommons.org/licenses/by-nc/4.0/>), which permits non-commercial re-use, distribution, and reproduction in any medium, provided the original work is properly cited. For commercial re-use, please contact [journals.permissions@oup.com](mailto:journals.permissions@oup.com)

- 14 Translational Neuroradiology Section, National Institute of Neurological Disorders and Stroke, National Institutes of Health (NIH), Bethesda, MD, USA
- 15 Neuroimaging Research Unit, Department of Neurology, Medical University of Graz, Graz, Austria
- 16 Section of Neuroradiology (Department of Radiology), Vall d'Hebron University Hospital and Research Institute, Barcelona, Spain
- 17 Department of Neurology, Cedars-Sinai Medical Center, Los Angeles, California, USA
- 18 Queen Square multiple sclerosis Centre, Department of Neuroinflammation, Queen Square Institute of Neurology, University College London, London, UK
- 19 Department of Brain and Behavioural Sciences, University of Pavia, Pavia, Italy
- 20 Brain MRI 3T Research Centre, IRCCS Mondino Foundation, Pavia, Italy

Correspondence to: Cristina Granziera  
 Neurology, University Hospital Basel,  
 Department of Biomedical Engineering,  
 University of Basel  
 Basel, Switzerland  
 E-mail: cristina.granziera@usb.ch / cristina.granziera@unibas.ch

**Abbreviations:** AD = axial diffusivity; DTI = diffusion tensor imaging; FA = fractional anisotropy; MD = mean diffusivity; MP2RAGE = magnetization prepared 2 rapid acquisition gradient echoes; MTR/sat = magnetization transfer ratio/saturation; MWF = myelin water fraction; QSM = quantitative susceptibility mapping; RD = radial diffusivity; T<sub>1</sub>-RT = T<sub>1</sub> relaxation time

## Introduction

Conventional MRI provides invaluable information for the diagnosis, prognosis, and monitoring of the effectiveness of therapeutics in patients with multiple sclerosis.<sup>1,2</sup> The term conventional MRI encompasses the methods used in clinical practice to describe pathology by relying on contrast changes in weighted images. These are images that predominantly, but not exclusively, reflect a biophysical contrast mechanism (e.g. T<sub>1</sub>- and T<sub>2</sub>-weighted scans). Using conventional MRI in the multiple sclerosis clinic, it is generally possible to identify the number, location, and activity of multiple sclerosis lesions, although the sensitivity to those characteristics generally varies depending on several technical factors.<sup>3</sup> On the other end, conventional MRI is largely insensitive to the heterogeneity of focal multiple sclerosis lesions and to the pathology affecting CNS tissue outside multiple sclerosis lesions (normal-appearing white and grey matter). Furthermore, conventional MRI is unable to depict the level of damage within different CNS tissue components, such as myelin, axons, and glia.

Better quantification of the extent, type, spatial distribution, and evolution over time of CNS tissue damage in patients with multiple sclerosis could improve our understanding of disease mechanisms. It may also aid in stratification of disease burden, assessment of therapy response and evaluation of subclinical disease progression.

Quantitative MRI can potentially address these needs by providing more sensitive measures of multiple sclerosis pathology and more specific information regarding which tissue component has been damaged (Fig. 1). Unlike conventional MRI, which acquires datasets that have a mixture of weightings and therefore cannot be resolved into a quantitative map, quantitative MRI relies exclusively on acquisitions that can then be used to disentangle the source of signal variations. Moreover, through computational or mathematical

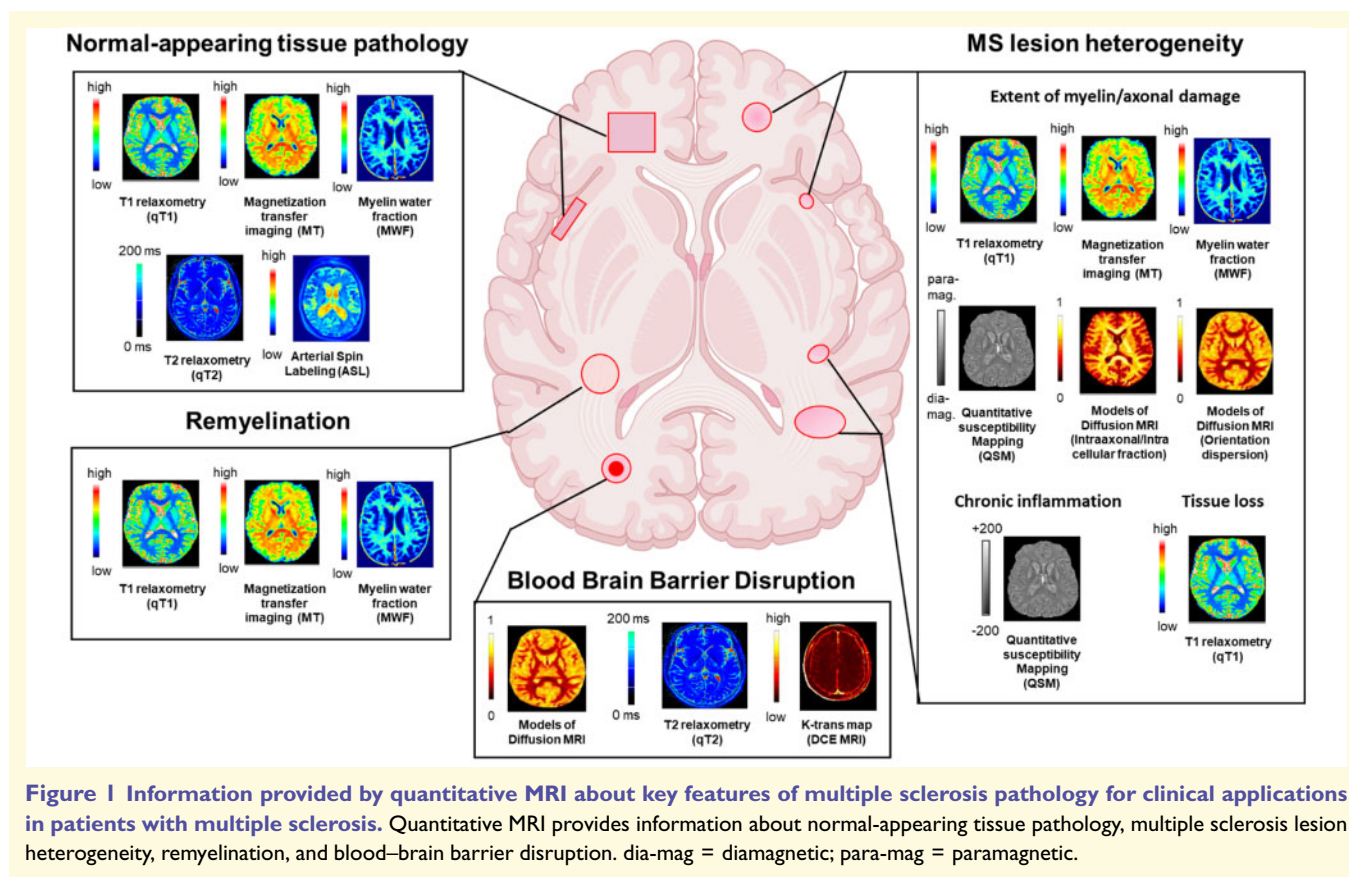
modeling, this approach can provide quantitative maps where intensities have physical units.<sup>4</sup> Thus, quantitative MRI techniques are superior to conventional MRI regarding their sensitivity to subtle alterations within lesions and normal-appearing tissue<sup>4</sup> as well as their increased specificity relating to the damage of different tissue components of the CNS (e.g. myelin, axons, glia, iron and blood flow/volume).

Nonetheless, quantitative MRI is not currently used in clinical practice, primarily because it has not reached 'clinical maturity'. A method can be considered 'clinically mature' when it can be run on most up-to-date clinical scanners without the need for additional sequence development, there is available and validated software able to process the data and provide the user with the desired quantitative maps, and cut-off values of pathology assessed with that method have been established.

In this review, we summarize: (i) the information that can, and cannot, be provided by conventional MRI; (ii) the contribution of quantitative MRI to our understanding of multiple sclerosis pathology in the brain and spinal cord; (iii) the relationship between quantitative MRI features and clinical outcome and the potential role of quantitative MRI in improving the prediction of disability, especially motor and cognitive deficits; and (iv) the clinical maturation stage of the various quantitative MRI techniques.

## Quantitative MRI and multiple sclerosis neuropathology

When radiographically investigating multiple sclerosis, conventional MRI provides the following measures: (i) number, volume, and location of focal T<sub>2</sub>-weighted hyperintense lesions; (ii) number of contrast-enhancing T<sub>1</sub>-weighted



lesions (CEL); (iii) number and volume of  $T_1$ -hypointense lesions (also called black holes); and (iv) global/regional volume of tissues (a measure of atrophy). However,  $T_2$ -weighted lesions are not pathologically specific, because they may represent active inflammation (e.g. oedema) as well as demyelination with or without axonal loss.  $T_1$ -hypointense lesions may also result from variable damage to different CNS tissue components (myelin/axon/cells), which cannot be distinguished. Therefore,  $T_2$ -weighted and  $T_1$ -hypointense lesions provide only basic information relating to the histopathological heterogeneity of multiple sclerosis lesions<sup>5,6</sup> and the different stages of lesion development and repair (e.g. remyelination) that may occur over time. Additionally, brain atrophy reflects only the late-stage results of degenerative phenomena and does not describe the normal-appearing tissue pathology preceding tissue volume loss. In fact, conventional MRI is mostly insensitive to the early and subtle axonal pathology,<sup>7</sup> alterations in myelin morphology (e.g. myelin blisters<sup>8</sup>) and early-stage dendrite/synapse changes such as those occurring in the hippocampus.<sup>9</sup>

## Quantitative MRI techniques

### $T_1$ relaxometry

$T_1$  relaxometry measures the recovery of longitudinal magnetization of excited spins in a tissue by providing  $T_1$

relaxation time ( $T_1$ -RT) values, which are related to the integrity of micro- and macrostructural components of a tissue<sup>10</sup> (Table 1).

### Pathological evidence

Several studies have explored the sensitivity and specificity of  $T_1$ -RT for detecting multiple sclerosis pathology (Table 1). The three major determinants of  $T_1$  changes in the CNS of patients with multiple sclerosis are myelin, iron, and water. While it is possible to model their effect on  $T_1$ -RT,<sup>11</sup> it is challenging to disentangle the relative contributions of myelin, axons, and free water (e.g. oedema in active lesions) to  $T_1$ -RT.<sup>12</sup> Indeed,  $T_1$ -RT highly correlates with both myelin ( $r = -0.78$ ,  $P < 0.001$ ) and axon content ( $r = -0.62$ ,  $P < 0.001$ ) within the normal-appearing white matter and within white matter lesions in the CNS.<sup>13</sup> Moreover, demyelination, axon loss, and iron loss may all lead to prolonged relaxation times.<sup>13,14</sup> Interestingly, lesions with longer  $T_1$ -RT are more destructive due to a combination of axonal loss and accumulation of extracellular water.<sup>15</sup> On the other hand, shortening or moderate prolongation of  $T_1$ -RT over time may suggest reparative phenomena such as remyelination and gliosis.<sup>16</sup>

### Assessment of multiple sclerosis impact and prognostic value

$T_1$ -RT mapping displays high accuracy for discriminating focal lesions in both white and cortical grey matter in

**Table 1** Technical background and pathological specificity and sensitivity of quantitative MRI techniques

Quantitative MRI technique	Contrast mechanism	Measure(s)	Specificity to multiple sclerosis pathology	Sensitivity to multiple sclerosis pathology
qT <sub>1</sub>	Recovery of longitudinal magnetization	T <sub>1</sub> -RT/R <sub>1</sub>	Low: myelin/axons/cells/macro- and micro molecules/water)	High: (lesions and NAT)
T <sub>2</sub> relaxometry	Loss of spin Coherence of water pools (myelin layers, intracellular, intra-axonal, extracellular)	T <sub>2</sub> -RT/R <sub>2</sub>	Low: myelin/axons/cells/water)	High: (lesions and NAT)
MWI	Loss of spin coherence of water molecules trapped in myelin	MWF	High: myelin	High: (lesions and NAT)
MTI	Exchange of magnetization between free protons and macromolecular protons (proteins/lipids)	MTR	Low: myelin/macromolecules (e.g. lipid/protein in biological membranes) extracellular water	High: (lesions and NAT)
DTI	Diffusivity of water proteins (intra-cellular-extracellular)	MD, RD/AD, FA	Low Highly dependent on tissue structure (e.g. fibre crossing/activated microglia/cells)	High: (lesions and NAT)
Diffusion-based models of microstructure	Modelling of water compartments Modelling of the diffusion magnetic resonance signals	Restricted water fraction (CHARMED) Axon calibre (ACTIVEX) Diffusion Kurtosis ICVF ODI fis	High ODI: neurite dispersion Moderate NDI: myelin and axonal count fis: Neurite and soma	High: (lesions and NAT, little evidence)
QSM	Local changes in tissue composition cause frequency shifts (measured by phase images)	Magnetic susceptibility	Low: Influenced by changes in iron/myelin/water content	Moderate: (lesions)
Perfusion MRI				
ASL	Magnetically labelled blood is used as endogenous tracer	CBV CBF	Moderate: linked to mitochondrial energetic failure; linked to elevated levels of endothelin-1	Moderate: (NAT)
DSC	Susceptibility effect of the paramagnetic contrast agent leads to signal loss in T <sub>2</sub> /T <sub>2</sub> *-weighted images	MTT K <sub>trans</sub> V <sub>e</sub>		
DCE	Wash-in, plateau, wash-out of contrast enhancement	V <sub>p</sub>		

The evaluation of 'specificity' and 'sensitivity' of quantitative MRI measures has been made along two criteria: (i) the strength of correlation between quantitative MRI measures with a given neuropathological feature (specificity); and (ii) the number of neuropathological features measured with quantitative MRI (sensitivity). Based on those criteria, an expert consensus was reached among the participants of the MAGNIMS workshop (Basel, December 2019) on 'Quantitative MRI towards clinical application in MS'. ASL = arterial spin labelling; CBF = cerebral blood flow; CBV = cerebral blood volume; DCE = dynamic contrast-enhanced; DSC = dynamic susceptibility contrast; fis = soma signal fraction; GM = grey matter; GRASE = gradient and spin echo; ICVF = intracellular volume fraction; K<sub>trans</sub> = transfer constant; MTI = magnetization transfer imaging; MTT = mean transit time; MWI = myelin water imaging; NDI = neurite density index; ODI = orientation dispersion index; V<sub>e</sub> = fractional volume of the extracellular space; V<sub>p</sub> = fractional volume of the plasma space.

patients with multiple sclerosis.<sup>17,18</sup> Ultra-high-field (7 T), T<sub>1</sub>-RT mapping can identify cortical focal pathology in cerebral hemispheres<sup>19</sup> and cerebellum<sup>20</sup> of patients with multiple sclerosis. In addition, whole-brain T<sub>1</sub>-RT maps at 3 T provide a personalized approach with which to assess the heterogeneity of damage in focal lesions and the extent of diffuse pathology by quantifying the changes in T<sub>1</sub>-RT compared to the normal distribution of T<sub>1</sub>-RT in healthy subjects.<sup>21</sup> T<sub>1</sub>-RT mapping studies have been used to generate whole-brain assessments of multiple sclerosis disease impact and progression. These studies found that global T<sub>1</sub>-RT increases with disease progression, predominantly in later disease stages and also correlates with brain atrophy.<sup>22,23</sup> The volume of lesions with very long T<sub>1</sub>-RT (black holes) better correlates with composite clinical functional scores

compared with total lesion volume,<sup>24</sup> and the decrease over-time in T<sub>1</sub>-RT inside black holes is associated with clinical improvement<sup>25</sup> and response to therapy.<sup>25</sup> Finally, patterns of T<sub>1</sub>-RT change associated with cognitive impairment can be observed even at early multiple sclerosis stages.<sup>26</sup>

### Technology availability in the clinic

To date, T<sub>1</sub> relaxometry has not been included in clinical multiple sclerosis protocols. There are several reasons for this: (i) numerous approaches have been proposed, exhibiting variable sensitivity to spurious effects such as magnetization transfer (MT), T<sub>2</sub> relaxation, diffusion, and B1 variation; (ii) there is no consensus for the best T<sub>1</sub> mapping sequence<sup>27,28</sup>; (iii) obtaining high accuracy for T<sub>1</sub> mapping *in vivo* is still challenging<sup>29</sup> (e.g. T<sub>1</sub> relaxation in white

matter is double-exponential because of magnetization exchange with myelin-bound protons, but most available methods assume single-exponential relaxation); and (iv) the complexity of the  $T_1$  mapping techniques often results in lack of reproducibility<sup>30</sup> (Table 2).

Despite challenges with reproducibility of  $T_1$  relaxometry, there are some promising  $T_1$  mapping approaches combining ‘clinically compatible’ scan times with high intra- and inter-scanner reproducibility. One of these is the magnetization prepared 2 rapid acquisition gradient echoes (MP2RAGE) sequence,<sup>31</sup> which has been shown to provide highly reproducible  $T_1$ -RT maps (3% coefficient of variability, CV) in a single-vendor, multicentric study<sup>32</sup> and in a  $T_1$  phantom study (NIST, National Institute of Standards and Technology) across different 3 T scanners.<sup>33</sup> MP2RAGE  $T_1$  maps provide a promising ‘all-in-one’ candidate for clinical practice, but achieving this will require manufacturers to collaborate to provide similar acquisitions across different scanners. In addition, clinical cut-offs of pathological changes in MP2RAGE maps still need to be defined. Another interesting approach is synthetic MRI (SyMRI<sup>®</sup>), which simultaneously analyses  $T_1/T_2$  relaxometry and proton density.<sup>34</sup> The SyMRI sequence and the software to reconstruct SyMRI maps can be implemented across scanners from all major vendors. Further, quantitative MRI maps can either be generated within a minute of the acquisition or can be installed as a call button on picture archiving and communication systems.<sup>35</sup> Moreover, SyMRI showed less than 6% variability in  $T_1$ -RT across scanners from different vendors.<sup>36</sup>

Interestingly, MP2RAGE  $T_1$  mapping has been recently reported in the spinal cord in < 10 min, with a maximum CV of 5%.<sup>37</sup>

## $T_2$ relaxometry, myelin water fraction, and magnetization transfer imaging

Myelin-sensitive metrics are essential to investigate multiple sclerosis pathophysiology<sup>38,39</sup> (Fig. 1), perform outcome predictions,<sup>40,41</sup> and assess therapeutic effects.<sup>42,43</sup>

Single-component  $T_2$  relaxometry (qT2) is obtained by fitting a single exponential and provides measures of  $T_2$ -RT that are sensitive to global water content in the CNS (intra/extracellular water and myelin water). Nevertheless, since  $T_2$  decay in the CNS tissue is largely multi-exponential, single-component qT2 is highly dependent on sequence parameters and noise<sup>44,45</sup> (Table 1).

The distinction of different water pools, including the myelin water pool [e.g. myelin water fraction (MWF)], in the CNS may be achieved by using multi-component  $T_2$  relaxometry<sup>46</sup> (Table 1). MT imaging exploits the selective saturation of protons bound to macromolecules, including myelin, and reduces their longitudinal magnetization. This renders it possible to create MT saturation images (MTsat) and magnetization transfer ratio (MTR) images providing information about this pool of molecules<sup>13</sup> (Table 1).

Single-component  $T_2$ -RT, MWF, and MTR are also sensitive to the relative presence of extracellular water. For example, their values may be influenced by the presence of oedema<sup>44,47</sup> (Table 1).

Other techniques, such as rapid estimation of myelin for diagnostic imaging (REMyDI), which is derived from SynMRI, can also be used to assess myelin integrity. REMyDI quantifies myelin by estimating its fast relaxation rate through magnetization exchange and effects on the observable proton pool (i.e. cellular water, free water, and excess parenchymal water partial volumes).<sup>34,48</sup>

### Pathological evidence

Myelin-related measures exhibit different specificity in regard to myelin content and myelin-related pathology in multiple sclerosis.

Post-mortem single-component  $T_2$  relaxometry in the normal-appearing tissue of the cervical spinal cord of patients with multiple sclerosis is highly influenced by demyelination ( $r = 0.77$ ,  $P < 0.001$ ) but does not seem to be strongly related to axonal damage ( $r = -0.44$ ,  $P < 0.001$ ).<sup>49</sup> Additionally, qT2 shows a strong linear correlation with iron concentration in healthy brains ( $r^2 = 0.67$ ,  $P < 0.001$ ).<sup>50</sup>

MWF shows strong correlations with myelin staining in both lesions and normal-appearing tissue in histological

**Table 2** Current state of reproducibility and availability for use in humans

Quantitative MRI technique	Inter-scanner reproducibility	Hardware/software availability for clinical use
qT <sub>1</sub>	Moderate High (MP2RAGE)	Limited
$T_2$ relaxometry	Moderate	Limited
MWI	High (little evidence)	Limited
MTI	Low/moderate	Limited
DTI	Moderate	Broad
Models of diffusion-based microstructure	Moderate (little evidence)	Limited
QSM	High (little evidence)	Limited
Perfusion MRI (ASL, DSC, DCE)	High	Broad

Reproducibility (inter-scanner and same field strength): high = < 5% coefficient of variation (CV); moderate = 5–15% CV; low = > 15% CV in reported studies. ASL = arterial spin labelling; DCE = dynamic contrast-enhanced; DSCE = dynamic susceptibility contrast; MTI = magnetization transfer imaging; qT<sub>1</sub> = quantitative  $T_1$ .

specimens of human brain (on average in lesions and normal-appearing tissue:  $r^2 = 0.67$ ,  $P < 0.0001$ ).<sup>46,51</sup> Whether MWF is also sensitive to accumulation of extracellular iron remains to be demonstrated. A recent post-mortem study attempted to answer this question by imaging brain specimens with two different techniques measuring MWF [Carr Purcell Meiboom Gill (CPMG), and gradient and spin echo (GRASE)], before and after a de-ironing procedure.<sup>52</sup> This work concluded that both were sensitive to brain iron content; however, this conclusion should be taken with caution, since the applied de-ironing procedure may well have affected the iron content within myelin and, as a consequence, altered myelin properties. Therefore, more studies are warranted to better understand the effect of extracellular iron on quantitative MRI techniques measuring MWF.

MTR, but not MTsat, has been validated by post-mortem studies and shows high correlations with myelin ( $r = 0.84$ ,  $P < 0.001$ )<sup>53</sup> and axon density ( $r = 0.83$ ,  $P < 0.0001$ )<sup>54</sup> when lesions and normal-appearing tissue are considered together. In addition, very recent MRI-pathology studies demonstrate that MTR sampled in lesion and non-lesion tissue in multiple sclerosis brains is weakly associated not only with myelin density [coefficient (95% confidence interval, CI): 0.31 (0.07 to 0.55),  $P = 0.01$ ], but also with greater numbers of astrocytes [coefficient (95% CI): 0.51 (0.02 to 1),  $P = 0.04$ ] and damaged mitochondria [coefficient (95% CI): 0.53 (−0.95 to −0.12),  $P = 0.01$ ].<sup>55</sup>

Amongst the most recent myelin-sensitive approaches, REMyDI myelin quantification was shown to weakly correlate with both proteolipid protein (PLP) immunostaining and Luxol fast blue staining in multiple sclerosis lesions but not with the same staining in normal-appearing white matter (multiple sclerosis lesions:  $0.02 < r < 0.48$ ,  $P < 0.001$ ).<sup>56</sup>

### Assessment of multiple sclerosis impact and prognostic value

In patients with short disease duration (i.e. <6 years), T<sub>2</sub>-RT values were increased in normal-appearing white matter<sup>57-59</sup> and normal-appearing grey matter<sup>60</sup> as compared to healthy controls. T<sub>2</sub>-RT in combination with diffusion MRI appeared to be sensitive also to extracellular water accumulation due to blood–brain barrier disruption in gadolinium-positive lesions, which could be identified with 85% accuracy using these two measures.<sup>61</sup> Similarly, MWF increased over 6 months following the appearance of enhancing lesions, as expected in repairing tissue.<sup>62</sup> Additionally, MWF was reported to be lower in lesions with paramagnetic rims compared with rim-negative lesions,<sup>63</sup> showing the more pronounced demyelination in the former lesion type. Also, MWF moderately decreased over time (−8%) in the normal-appearing white matter of a small group of patients followed over an average period of 5 years. Global MWF was likewise abnormal in the brain and cervical spinal cord of patients with primary progressive multiple sclerosis compared to controls,<sup>64</sup> and, when followed for 2 years, decreased at the C2–C3 spinal cord

level<sup>65</sup>; moreover, cervical spinal cord MWF showed an association with disability.<sup>65</sup>

MTR changes in normal-appearing white matter preceded the appearance of gadolinium-enhancing lesions in patients with multiple sclerosis<sup>66</sup> and recovered following the acute phase,<sup>67</sup> especially in treated patients.<sup>68</sup> MTR was significantly lower in hypointense lesions as compared with isointense lesions on T<sub>1</sub>-weighted images at the time of initial enhancement.<sup>69</sup> For lesions that changed from hypointense to isointense, MTR increased significantly during 6 months of follow-up.<sup>69</sup> Intralesional MTR showed longitudinal changes consistent with demyelination and remyelination in different regions of active lesions in the 3 years following treatment.<sup>70</sup> MTR also appeared to be lower in outer compared to inner cortical layers in the brain, and in the subpial region compared to the central region in the spinal cord<sup>71</sup>; this may be consistent with differences in myelin content, but may also, at least in part, be due to partial volume effects. The lowest outer cortical MTR was seen in secondary progressive multiple sclerosis and is consistent with more extensive outer cortical (including subpial) pathology.<sup>72</sup> MTR abnormalities in the subpial region, in both brain and spinal cord, occurred early in the course of multiple sclerosis and were more marked in patients with a progressive disease course.<sup>73</sup> As for the spinal cord, lower MTR values were found in the cervical cord of patients with RRMS<sup>71,74</sup> and primary progressive multiple sclerosis<sup>74</sup> compared to controls, which further decreased over 5 years follow-up.<sup>74</sup>

In contrast to MTR, MTsat has been evaluated in patients with multiple sclerosis in a few studies, revealing its sensitivity to normal-appearing white/grey matter abnormalities<sup>75,76</sup> and multiple sclerosis lesions.<sup>76,77</sup> A proper comparison between the sensitivity of MTsat and MTR to multiple sclerosis pathology has still to be performed, but there is preliminary evidence that MTsat in the cervical spinal cord better correlates with disability than MTR.<sup>78</sup>

Myelin maps provided by REMyDI showed increased myelin loss in normal-appearing white matter of patients with multiple sclerosis compared to controls, which correlated with baseline cognitive and physical disability.<sup>56</sup> Longitudinally, MWF correlated with follow-up physical disability, even after adjusting for baseline disability.<sup>56</sup>

### Technology availability in the clinic

Up to now, MTR/MT sat, qT2, and MWF have not been available for clinical use (Table 2). However, there are now some sequences that provide qT2 and MWF maps in 3–6 min, a time that may be compatible with clinical protocols.<sup>79-82</sup> Similarly, for the cervical spinal cord, fast acquisitions for MWF begin to be available.<sup>83</sup>

There are also several sequences available to perform MT imaging, but none can provide the reconstruction of MTR maps in a clinical setting. Interestingly, the comparison of different myelin-sensitive methods (GRASE- and mcDESPOT-MWF, qT1, and MTR) indicates that the type of sequence needs to be chosen according to the purpose of its application. For example, the GRASE sequence should be

used when the greatest confidence is required for assessing changes specific to myelin.<sup>39</sup> If sensitivity to lesion and normal-appearing white matter pathology is the priority, then mcDESPOt-MWF and qT1 are the most sensitive approaches.<sup>39</sup>

Although achieving reproducible MTR measurement has traditionally been challenging, by carefully controlling the sources of technical variability (protocols, type of coil for MT saturation, and B1 inhomogeneities), it is feasible to obtain inter-scanner MTR in healthy controls, the variability of which lies within the mean inter-subject variability.<sup>84,85</sup> Also, MTsat exhibits moderate variations [CV intra-scanner 7–12%; CV inter-scanner: 15.7% (<5% if MT harmonization is performed)].<sup>86</sup>

Intra-scanner reproducibility of MWF in white matter is quite high ( $r = 0.95$ – $0.99$ ),<sup>81,82,87</sup> and the same holds true in small areas simulating multiple sclerosis lesions ( $r = 0.89$ )<sup>62</sup>. Slightly lower, but still very good, is the inter-scanner and inter-vendor reproducibility for some myelin water imaging sequences in white matter ( $r = 0.91$ , CV < 3%<sup>88</sup>) although more studies are required to elucidate this aspect also for other ‘clinically compatible’ MWI sequences.

An initial assessment of reproducibility of myelin maps as provided by SyMRI, including REMyDI, showed moderate reproducibility across vendors ( $\rho = 0.89$ ).<sup>76</sup>

In the spinal cord, measurement errors for MTR and MTsat remain very large,<sup>89</sup> and more data are required to understand the intra- and inter-scanner reproducibility of fast spinal MWF acquisitions.

## Diffusion microstructure

Diffusion MRI probes CNS tissue integrity using metrics derived from modelling signal changes associated with the diffusion of water molecules in tissue, which can characterize cellular compartments of brain tissue within multiple sclerosis lesions, normal-appearing white matter, and normal-appearing grey matter (Table 1 and Fig. 1).

Diffusion tensor imaging (DTI) is a technique widely available in clinical research and clinical practice. DTI-derived metrics [fractional anisotropy (FA), radial/axial diffusivity (RD/AD), and mean diffusivity (MD)/apparent diffusion coefficient (ADC)] have been used for many years to assess the CNS tissue integrity in both regions of interest and along specific white matter tracts.<sup>90–93</sup> Beyond DTI, several mathematical models and computational approaches have attempted to decode the information contained in diffusion-weighted signals to retrieve specific features of tissue microstructure by: (i) modelling the tissue (e.g. tissue geometry and water dispersion) and associated signals; or (ii) computationally exploring the magnetic resonance signal (e.g. assessing signal behaviour with minimal or no underlying geometrical assumptions). Some models have attempted to separate different water compartments (extracellular, intracellular, and other) within CNS tissue.<sup>94</sup> These approaches normally require diffusion acquisitions that are more complex than the ones clinically used for DTI, encompassing

multiple b-values and sampling the signal in numerous directions. Extensive work comparing different diffusion-weighted imaging models and their ability to explain acquired data demonstrated that on average, and with the methods tested, tissue models tend to explain diffusion-weighted signal behaviour better than do signal models.<sup>95</sup>

The composite hindered and restricted model of diffusion (CHARMED) separates the intra- and extracellular water compartments and generates maps of the restricted water fraction (FR), a proxy for axon density.<sup>96</sup> The CHARMED framework has been extended to account for different axonal diameters, providing the opportunity to map the distribution of axon diameters within the brain using AxCaliber<sup>97,98</sup> or ActiveAx<sup>99</sup> frameworks. Another method is diffusion kurtosis imaging (DKI), which aims to provide a more accurate model of diffusion-weighted signal changes capable of capturing non-Gaussian diffusion behaviour as a reflection of tissue heterogeneity.<sup>100</sup> Diffusion-based spectrum imaging (DBSI) models the diffusion signal as a linear combination of anisotropic diffusion tensors reflecting fibres, which are predominantly axon fibres in white matter, and a spectrum of isotropic diffusion tensors that encompass cells, oedema, and CSF.<sup>101,102</sup>

Neurite orientation dispersion and density imaging (NODDI) is a three-compartment tissue model providing metrics to measure the intracellular volume fraction (ICVF) or neurite density index (NDI) and the orientation dispersion index (ODI), which describe intracellular diffusion in terms of neurite density and the degree of fibre dispersion of neurites, respectively.<sup>103</sup> Soma and neurite density imaging (SANDI) is another tissue-model aimed at further distinguishing the intracellular space by separately modelling the intra-neurite and intra-soma spaces.<sup>104</sup>

Q-space imaging may be applied to study the microstructural changes in white matter by estimating the water diffusion function, the probability density function (PDF), also called mean apparent propagator (MAP)<sup>105</sup> or ensemble average propagator (EAP).<sup>106,107</sup>

## Pathological evidence

Post-mortem studies showed that DTI-derived FA and MD in normal-appearing white matter correlate to myelin content ( $r = -0.79$  and  $r = 0.68$ ,  $P < 0.001$  for both) and to a lesser degree axon count ( $r = -0.7$  and  $r = 0.66$ ,  $P < 0.001$  for both).<sup>108</sup> Also, in the cortex of non-neurological subjects and patients with multiple sclerosis, FA values strongly relate to axon density [ $\beta$  (95% CI) = 1.56 (0.69 to 2.44) and  $\beta$  (95% CI) = 0.93 (0.45 to 1.42),  $P < 0.05$  for both] but not to myelin, glia, and total cell density.<sup>109</sup> However, these results should be taken with caution as the relationship between DTI parameters and myelin/axon content decreases in lesions and varies in regions of complex microstructure (e.g. crossing fibres<sup>110–113</sup>).

Post-mortem validation of microstructural features derived from biophysical diffusion models has been performed for some models. However, very few of these models have been evaluated in multiple sclerosis tissue specimens. AxCaliber

showed a very high agreement between the estimated axon diameter distribution in various nerve samples and axon diameter histograms on histology images ( $r = 0.98$  for optic nerve and  $r = 0.86$  for sciatic nerve<sup>97</sup>). ActiveAx maps of axon diameter and density indices exhibited a similar distribution pattern to those observed histopathologically in the corpus callosum and corticospinal tract.<sup>99</sup> NODDI ODI has been reported to correspond well with histological measures of neurite orientation dispersion in brain and spinal cord (controls:  $r = 0.84$ ;  $P < 0.001$ ; multiple sclerosis:  $r = 0.60$ ;  $P = 0.001$ ), whereas NODDI NDI showed good correlation with myelin ( $r = 0.74$ ;  $P < 0.001$ ) and moderate correlation with histology-derived neurofilament density measures ( $r = 0.56$ ;  $P = 0.002$ ).<sup>114,115</sup> In post-mortem specimens of multiple sclerosis lesions in the spinal cord, lower NDI and increased ODI were observed compared to non-lesion tissue.<sup>114</sup> Also, in the same specimens, NDI was reported to be sensitive to myelin and axon count.<sup>114</sup> As to DBSI, the study of one biopsied tumefactive multiple sclerosis lesion showed that DBSI-derived AD better detected axonal loss than DTI<sup>116</sup> but no correlation between DBSI parameters and axonal density was reported.

Other emerging microstructural diffusion models still require histopathological validation in healthy controls and multiple sclerosis brain specimens.

#### Assessment of multiple sclerosis impact and prognostic value

Even though DTI measures provide only a coarse approximation of CNS tissue properties, they have been extensively used in multiple sclerosis research studies. Increases in MD/ADC have been reported up to 6 weeks before contrast enhancement,<sup>117,118</sup> and MD in enhancing lesions has been shown to be much lower than in non-enhancing lesions.<sup>119</sup> Increased MD in acute multiple sclerosis lesions also appeared to predict risk of developing persistent black holes.<sup>120</sup> Furthermore, DTI measures along white matter tracts showed a progressive increase in MD in patients with no evidence of clinical or radiological disease-activity,<sup>121</sup> and a decrease in RD as well as an increase in AD in progressive patients with multiple sclerosis.<sup>91</sup> In addition, the peak width of skeletonized MD appeared to be higher in RRpatients with multiple sclerosis compared to controls.<sup>122</sup> Recent DTI studies in the cervical spinal cord have reported increased RD and reduced FA in RRMS with acute spinal cord involvement, when compared with healthy controls, and in SPMS, when compared with clinically stable RRMS.<sup>123,124</sup>

DTI metrics in the brain can also predict disability progression<sup>125</sup> and cognition,<sup>126</sup> especially in combination with clinical variables.<sup>127</sup> Likewise, RD in the optic nerve is inversely related to visual acuity in patients with multiple sclerosis<sup>128</sup> and has been shown—together with FA—to correlate with clinical disability in patients with spinal cord lesions.<sup>124,129</sup> Furthermore, baseline RD in the cervical spinal cord over a 6-month period during an acute cord relapse correlates with recovery at 6 months.<sup>130</sup> Also, FA

and MD change over time in patients with multiple sclerosis, but those measure do not seem to relate to changes in disability.<sup>131</sup>

DKI measures (e.g. mean kurtosis) are affected in patients with multiple sclerosis compared to controls<sup>132</sup> and are related to patient's disability.<sup>133</sup> DBSI-derived measures in white matter lesions and in the corpus callosum distinguished clinical multiple sclerosis subtypes with moderate accuracy<sup>134</sup> and also different types of multiple sclerosis lesions.<sup>135</sup>

The CHARMED-derived restricted water fraction is decreased in early multiple sclerosis, both in lesions and in normal-appearing white matter,<sup>136</sup> and decreases over time in lesions and normal-appearing white matter.<sup>137</sup> NODDI shows a lower neurite density (NDI) together with a higher neurite orientation dispersion (ODI) in normal-appearing white matter and in multiple sclerosis lesions compared with healthy white matter, both in the brain<sup>137–139</sup> and in the cervical spinal cord.<sup>114,140,141</sup> NODDI abnormalities are more pronounced in patients with SPMS than RRMS.<sup>139</sup> Additionally, NODDI measures better correlate with disability and cognitive/motor function in patients with multiple sclerosis than do standard DTI metrics.<sup>139</sup>

Last,  $q$ -space imaging (QSI) perpendicular diffusivity is higher and parallel diffusivity lower in the cervical spinal cord of progressive PPMS compared to healthy subjects,<sup>142</sup> and those changes become more evident over time.<sup>143</sup> Also, an increase in cord QSI indices of perpendicular diffusivity is associated with disability worsening over 3 years in PPMS.<sup>143</sup>

#### Technology availability in the clinic

Currently, DTI protocols are available for most clinical scanners and could be used in clinical practice, although DTI measures are more often used for comparisons between patient groups in research studies than for management of individual patients. More studies are needed to better understand the clinical validity of DTI-derived metrics for patients with multiple sclerosis.<sup>110</sup>

Reproducibility of DTI metrics has been assessed in numerous studies, which showed that FA has an intra-scanner coefficient of variation  $< 3\%$  and MD 0–7%, whereas the inter-scanner coefficient of variability for both FA and MD is reported to be  $\leq 5\%$ .<sup>144–150</sup> Nevertheless, further studies should assess DTI reproducibility in multiple sclerosis cohorts.

Microstructural models applied to multi-shell diffusion data are far from being ready for clinical adoption, and only few reproducibility studies have been performed. Among those, some works reported an inter-vendor reproducibility of NODDI ranging from 2.3% to 14% and an intra-scanner reproducibility  $\leq 4\%$ .<sup>151,152</sup> More works are required to understand the potential clinical role of microstructural metrics and their reproducibility across scanners and vendors.

As for the spinal cord, a recent investigation of the reproducibility of DTI-derived measures at C1–C6 between different sites has shown the feasibility of multicentre spinal cord



DTI, when sequence parameters are homogenized across sites and vendors.<sup>153</sup>

## Quantitative susceptibility mapping

Quantitative susceptibility mapping (QSM) encompasses imaging methods by which the absolute concentrations of iron, calcium, myelin, and other substances may be measured in tissues based on their changes in local magnetic susceptibility (Table 1). In particular, the magnetic susceptibility is calculated from local frequency shifts in the MRI signal of a gradient echo sequence (as obtained from the phase images) through deconvolution with a dipole kernel. Several methods have been proposed to solve this ill-posed inverse problem.<sup>154</sup> QSM maps can quantify paramagnetic trace elements, such as iron in ferritin, deoxygenated-heme in the blood, and diamagnetic calcium. In addition, myelin<sup>155</sup> and the microstructural anisotropy of white matter<sup>156–159</sup> can also induce local shifts of the magnetic susceptibility because of the diamagnetism of proteins and lipids.<sup>160</sup> QSM also provides an improved contrast-to-noise ratio for certain tissues and structures compared with  $T_2^*$ -weighted magnitude images. However, because of phase filtering, QSM does not provide absolute susceptibility values, and, therefore, QSM is computed in relationship to a reference region.<sup>161</sup> Moreover, the magnetic susceptibility in white matter is a tensor (i.e. it depends on fibre orientation with respect to the main magnetic field,  $B_0$ ), which can make the interpretation of susceptibility changes in white matter challenging.<sup>162</sup>

### Pathological evidence

A post-mortem study before and after brain fixation at 7 T showed that QSM is positively related to ferritin iron content ( $r = 0.76$ ) and negatively related to myelin content ( $r = -0.35$ ), which indicates a paramagnetic effect of iron and a diamagnetic effect of myelin on tissue magnetic susceptibility.<sup>163</sup> In multiple sclerosis brain samples, QSM identifies iron accumulation in microglia and macrophages surrounding chronic active and smoldering lesions<sup>164,165</sup> as well as active myelin digestion during lesion formation.<sup>166</sup>

### Assessment of multiple sclerosis impact and prognostic value

QSM reveals magnetic properties sensitive to iron and myelin, and thus can capture specific characteristics of multiple sclerosis lesions (Fig. 1). Longitudinal QSM measurements in patients with multiple sclerosis have shown an initial large rise in magnetic susceptibility occurring within weeks in active lesions, and a subsequent increase that occurs for months.<sup>167</sup> The former has been attributed to myelin digestion and the latter to the removal of the myelin debris within macrophages and the release of iron.<sup>167</sup> In addition, lesions with higher susceptibility at the border and larger volume maintained a high magnetic susceptibility value for a number of years,<sup>167</sup> a finding confirmed by susceptibility-weighted imaging (SWI) at ultrahigh field.<sup>164</sup> These lesions are particularly interesting as they are thought to contain smoldering

inflammation and are associated with rapid clinical progression.<sup>168</sup> Magnetic susceptibility values in the basal ganglia were higher in patients with clinically isolated syndrome and multiple sclerosis than in control subjects.<sup>154</sup> Furthermore, this increased iron deposition in the basal ganglia, measured by QSM at 7 T, correlated with cognitive measures of inhibitory control in patients with multiple sclerosis.<sup>169</sup>

Magnetic susceptibility values from QSM maps showed promise in detecting enhancing lesions without the use of gadolinium.<sup>167</sup> Finally, QSM is also sensitive to the oxygenation state of blood, thereby allowing calculation of the oxygen extraction fraction. Thus, patients with multiple sclerosis were found to exhibit lower oxygen extraction fraction than controls, which is possibly related to mitochondrial dysfunction.<sup>170</sup>

### Technology availability in the clinic

It is relatively easy to collect data that may be used to reconstruct QSM maps on clinical MRI scanners. In fact, many clinical protocols are already applying 2D or 3D GRE (gradient echo) sequences to obtain  $T_2^*$ -weighted or SWI, and these protocols may also be used for QSM if phase images are available. Currently, the main hurdle for the broad translation of QSM into clinics is that MRI vendors have yet to implement the necessary algorithms on their commercial scanners. In addition, offline reconstruction of QSM maps is laborious and not easy to implement in routine clinical practice. Also, there is currently no consensus about which algorithm is best for QSM reconstruction. Most current QSM approaches suffer from over-smoothing and loss of conspicuity of fine features, as the methods are primarily optimized to minimize error metrics, not improve image quality.<sup>171</sup>

Brain QSM measurements performed by using the same algorithm in different magnetic resonance scanners exhibit: (i) excellent inter- and intra-scanner reproducibility for healthy subjects ( $r = 0.99$  and  $r = 0.98$ , respectively)<sup>172</sup>; (ii) very high intra-scanner reproducibility for patients with multiple sclerosis ( $r = 0.97$ )<sup>172</sup>; and consistently high intra- and inter-scanner reproducibility in phantoms with different gadolinium concentrations.<sup>173</sup>

To date, QSM has not been developed for spinal cord imaging.

## Perfusion imaging

Blood perfusion in the brain can be assessed using a tracer injection (e.g. gadolinium-based contrast agents) during the MRI acquisition of: (i) a  $T_2^*$ -weighted dynamic susceptibility contrast (DSC) sequence, which may provide relevant parameters in patients with multiple sclerosis such as: cerebral blood flow, cerebral blood volume, and mean transit time; or (ii) a  $T_1$ -weighted dynamic contrast enhancement (DCE) sequence able to measure the volume transfer constant  $K_{trans}$ , which is a measure of permeability between blood plasma and tissue extravascular spaces and of plasma blood flow and capillary surface area. Alternatively, arterial spin labelling (ASL), a technique which does not require intravenous administration

of gadolinium-based contrast agents, uses magnetically labelled blood as the intrinsic contrast agent, most commonly measuring cerebral blood flow and volume.

### Pathological evidence

Chronic hypoperfusion induces mitochondrial dysfunction leading to energetic failure and oxidative stress, which are increasingly recognized as crucial factors associated with axonal degeneration in multiple sclerosis.<sup>174</sup> Furthermore, generalized microstructural damage in normal-appearing white matter could be associated with elevated levels of endothelin-1, a vasospastic peptide.<sup>175</sup>

### Assessment of multiple sclerosis impact and prognostic value

Changes in local perfusion are known to precede the initial blood–brain barrier breakdown and T<sub>2</sub>-weighted lesion appearance by several weeks.<sup>176</sup> In general, lesions tend to develop preferentially in hypoperfused brain areas,<sup>177</sup> but the relation of hypoperfusion to T<sub>2</sub>-weighted lesion load is controversial.<sup>178–180</sup> Generalized hypoperfusion in normal-appearing white matter is correlated with microstructural damage in the brain parenchyma.<sup>174</sup> Brain perfusion is generally reduced in chronic disease phases,<sup>181,182</sup> is correlated with diffuse axon degeneration,<sup>174</sup> and precedes atrophy development.<sup>183</sup> Gliosis also induces less metabolic demand and results in decreased perfusion.<sup>176</sup> Reductions in cerebral blood volume and cerebral blood flow in multiple sclerosis are associated with worsening of physical disability<sup>184</sup> and have been widely reported to correlate with disability and composite functional scores.<sup>181,182,185–187</sup> Correlations with the mean transit time are still controversial, as this parameter is not consistently altered in multiple sclerosis as it is in other conditions such as stroke.<sup>185–187</sup> A multitude of studies have consistently described the correlation between cognitive decline and reduced perfusion parameters,<sup>180,188–191</sup> as well as with fatigue in multiple sclerosis.<sup>188,190,192</sup> Hypercapnic perfusion experiments showed impaired dilatory capacity of cerebral arterioles in multiple sclerosis in response to vasomotor stimulations.<sup>193</sup>

### Technology availability in the clinic

In general, perfusion data in multiple sclerosis may be hampered by sensitivity to artefacts, dependency on haematocrit, and the lack of absolute quantification, which may render difficult the interpretation and comparison of data acquired at different time points or across scanners.<sup>194–196</sup> Standardization of protocols and analyses is currently under development.

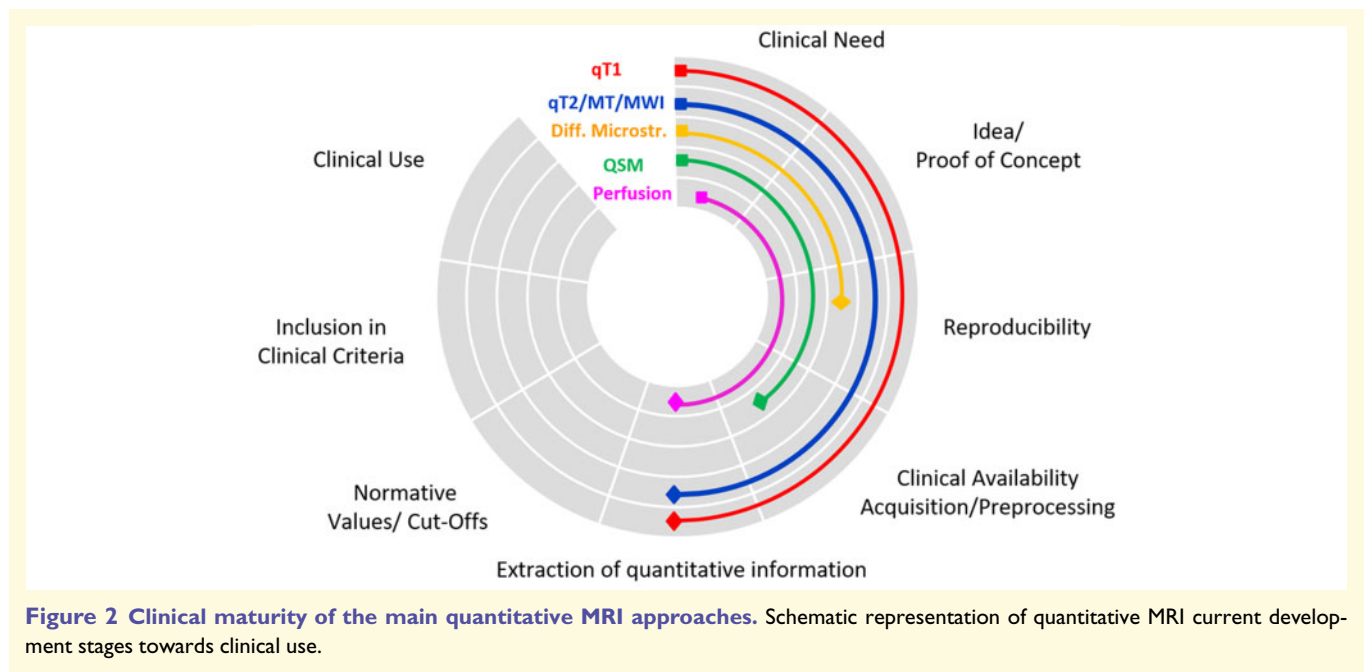
## Towards clinical application and clinical decision support with quantitative MRI

In theory, quantitative MRI techniques that measure accurately and reproducibly a biologically specific signal

correlating with, or predictive of, clinical outcomes, are ideal candidates for clinical applications. In practice, such techniques do not exist yet (Tables 1 and 2). Among the currently available quantitative MRI approaches, those achieving high accuracy (which usually comes at the cost of reproducibility) are extremely appealing for research investigating the underlying tissue changes; on the other end, those providing high reproducibility, acceptable accuracy, and good correlation with clinical measures, despite not comprehensively explaining clinical function or disability, may be useful for the management of people with multiple sclerosis or in assessing therapies for patients with multiple sclerosis.

Currently, quantitative MRI techniques lack some of the development steps necessary to achieve clinical maturity (Fig. 2). These include clinical availability of acquisition methods and tools to reconstruct parametric maps; methods to extract quantitative information from parametric maps; and normative values and pathological cut-offs (Fig. 2). Additionally, the clinical value of quantitative maps needs to be compared with existing diagnostic and prognostic criteria in the clinical setting. In this context, qT1 (e.g. MP2RAGE and SyMRI) and, to some extent, myelin imaging (e.g. SyMRI) appear to be the most technically advanced and ready for use in studies aimed at providing methods to extract quantitative information, either through brain and spinal cord atlases<sup>197–199</sup> or comparison of single subjects to large cohorts of healthy cohorts<sup>21</sup> (Fig. 2). Although brain myelin imaging may be ready for clinical adoption, we still lack software solutions that can provide clinicians with valuable information related to the state of damage or repair of the underlying tissue. QSM and diffusion-based methods providing microstructural information warrant further technological development, and their reproducibility must be assessed in a multicentre setting. Finally, while perfusion MRI may be considered to assess blood–brain barrier permeability and for monitoring disease progression, more studies are needed to provide evidence of its clinical value in multiple sclerosis.

Another important consideration is whether specific quantitative MRI methods are better suited for the characterization of specific multiple sclerosis disease subtypes, assessment of disease progression, and evaluation of therapy response. The data presented in this review suggest that, currently, T<sub>1</sub> relaxometry and QSM may be most suitable for multiple sclerosis stratification by contributing to the identification of lesions associated with more extensive tissue damage and to the differentiation of acute versus chronic inflammatory lesions. Myelin-sensitive quantitative MRI techniques [MTR/MTsat, myelin water imaging (MWI), and T<sub>2</sub> relaxometry] and diffusion-microstructure MRI measurements may be most appropriate for assessing clinical progression through the characterization of normal-appearing tissue abnormalities, and may also be used to evaluate therapy effects on specific CNS tissue components (e.g. myelin and axons). As quantitative MRI methods become better standardized, further studies will be required to define their role in the management of patients with multiple sclerosis.



Besides cerebral imaging, quantitative MRI (e.g. DTI, MTR/MTsat, and MWI) also holds promise for imaging of the spinal cord, but both additional software (for localization, gating, and motion compensation) and hardware development (e.g. multi-channel phased-array coils) are required to pave the path towards application of spinal quantitative MRI for multiple sclerosis management.

In summary, quantitative MRI has the potential to provide information that can improve patient stratification, assessment of therapy response, and evaluation of subclinical disease progression. Whether these techniques should be embedded in clinical routines or selected for targeted implementations and studies within the clinical arena is still to be determined. Future work should be targeted at improving quantitative MRI clinical maturity through multicentre collaborations.

## Funding

C.G. is supported by the Swiss National Science Foundation (SNSF) grant PP00P3\_176984, the Stiftung zur Förderung der gastroenterologischen und allgemeinen klinischen Forschung and the EUROSTAR E! 113682 HORIZON2020. F.B. is supported by the National Institute for Health Research biomedical research center at University College London Hospitals. J.W. is supported by the EU Horizon2020 research and innovation grant (FORCE, 668039). D.S.R. is supported by the Intramural Research Program of National Institute of Neurological Disorders and Stroke, National Institutes of Health. A.T.T. is supported by an Medical Research Council grant (MR/S026088/1). S.R. is supported by the

Austrian Science Foundation (FWF) grant I-3001. P.S. is supported by the Intramural Research Program of National Institute of Neurological Disorders and Stroke, National Institutes of Health. H.V. is supported by the Dutch multiple sclerosis Research Foundation, ZonMW and HealthHolland.

## Competing interests

C.G. The University Hospital Basel (USB), as the employer of C.G. has received the following fees which were used exclusively for research support: (i) advisory board and consultancy fees from Actelion, Novartis, Genzyme and F. Hoffmann-La Roche; (ii) speaker fees from Biogen and Genzyme-Sanofi; (iii) research support by F. Hoffmann-La Roche Ltd. Before employment at USB, C.G. received speaker honoraria and travel funding by Novartis. J.W. Employee of the Medical Image Analysis Center Basel, Switzerland; speaker honoraria (Bayer, Biogen, Novartis, Teva); advisory boards and research grants (Actelion, Biogen, Idorsia, Novartis, Roche, Sanofi-Genzyme). F.B. has received compensation for consulting services and/or speaking activities from Bayer, Biogen, Merck, Novartis, Roche, Teva, and IXICO and is supported by the NIHR Biomedical Research Centre at UCLH. M.C. has received honoraria from Roche, Biogen- Idec, Genzyme, Merck Serono, Novartis and Teva for consulting services, speaking, and travel support. He serves on advisory boards for Merck, Novartis, Biogen-Idec, Roche, and Genzyme. N.D. has received honoraria from Biogen- Idec, Genzyme, Merck Serono, Novartis, Roche, Celgene and Teva for consulting services, speaking, and travel support. He serves on advisory boards for Merck,

Novartis, Biogen-Idec, Roche, and Genzyme, Immunic and he has received research grant support from the Italian MS Society. C.E. has received funding for travel and speaker honoraria from Biogen, Bayer Schering, Merck Serono, Novartis, Shire, Genzyme and Teva Pharmaceutical Industries Ltd., Sanofi-Aventis; research support from Merck Serono, Biogen, and Teva Pharmaceutical Industries Ltd./Sanofi-Aventis; and has served on scientific advisory boards for Bayer Schering, Biogen, Celgene, Merck Serono, Novartis, Roche and Teva Pharmaceutical Industries Ltd./Sanofi-Aventis. N.E. has received funding for travel and speaker honoraria from Biogen, Roche and Merck Serono; and has served on scientific advisory boards for Biogen, Merck Serono, Novartis, and Roche. M.F. is Editor-in-Chief of the Journal of Neurology; received compensation for consulting services and/or speaking activities from Biogen Idec, Merck-Serono, Novartis, Teva Pharmaceutical Industries; and receives research support from Biogen Idec, Merck-Serono, Novartis, Teva Pharmaceutical Industries, Roche, Italian Ministry of Health, Fondazione Italiana Sclerosi Multipla, and ARiSLA (Fondazione Italiana di Ricerca per la SLA). J.J.G.G. received research support from Biogen, Novartis, and Genzyme. He is President of the Netherlands Organisation for Health Research & Development and is an editor at MS Journal. D.S.R. has received research support from Vertex Pharmaceuticals. M.A.R. received speakers' honoraria from Biogen Idec, Novartis, Genzyme, Sanofi-Aventis, Teva, Merck Serono and Roche and receives research support from the Italian Ministry of Health and Fondazione Italiana Sclerosi Multipla. S.R. has received honoraria from Axon Neuroscience, QPS, and NeuroScios for consulting services. A.R. serves on scientific advisory boards for Novartis, Sanofi-Genzyme, SyntheticMR, Bayer, Roche, Biogen, and OLEA Medical, and has received speaker honoraria from Bayer, Sanofi-Genzyme, Merck-Serono, Teva Pharmaceutical Industries Ltd, Novartis, Roche and Biogen. A.T.T. has received speaker honoraria from Biomedica, Sereno Symposia International Foundation, Bayer and meeting expenses from Biogen Idec and has been the UK PI for two clinical trials sponsored by MEDDAY pharmaceutical company [MD1003 in optic neuropathy (MS-ON) and progressive MS (MS-SPI2)]. H.V. has received research grants from Merck Serono, Novartis and Teva, speaker honoraria from Novartis, and consulting fees from Merck Serono; all funds paid directly to his institution. L.K. reported research support for his institution (University Hospital Basel), including steering committee, advisory board, and consultancy fees, from Actelion, Addex, Bayer HealthCare, Biogen, Biotica, Celgene/Receptos, Genzyme, Lilly, Merck, Mitsubishi, Novartis, Ono Pharma, Pfizer, Sanofi, Santhera, Siemens, Teva, UCB, and Xenoport; speaker fees from Bayer HealthCare, Biogen, Merck, Novartis, Sanofi, Teva; support of educational activities from Bayer HealthCare, Biogen, CSL Behring, Genzyme, Merck, Novartis, Sanofi, and Teva; and grants from Bayer HealthCare, Biogen, F. Hoffmann-La Roche Ltd, Merck, Novartis, the European

Union, the Roche Research Foundations, the Swiss Multiple Sclerosis Society, and the Swiss National Research Foundation. All other authors report no competing interests.

## Appendix I

Authors are members of the MAGNIMS network (Magnetic Resonance Imaging in multiple sclerosis; <https://www.magnims.eu/>), which is a group of European clinicians and scientists with an interest in undertaking collaborative studies using MRI methods in multiple sclerosis, independent of any other organization and is run by a steering committee whose members are: F. Barkhof (Amsterdam), N. de Stefano (Siena), J. Sastre-Garriga (Barcelona), O. Ciccarelli (London), C. Enzinger (Graz, Co-Chair), M. Filippi (Milan), Claudio Gasperini (Rome), L. Kappos (Basel), J. Palace (Oxford), H. Vrenken (Amsterdam), À. Rovira (Barcelona), M.A. Rocca (Milan, Co-Chair), and T. Yousry (London).

## References

1. Rovira A, Wattjes MP, Tintore M, et al. Evidence-based guidelines: MAGNIMS consensus guidelines on the use of MRI in multiple sclerosis-clinical implementation in the diagnostic process. *Nat Rev Neurol*. 2015;11:471-482.
2. Wattjes MP, Rovira A, Miller D, et al. Evidence-based guidelines: MAGNIMS consensus guidelines on the use of MRI in multiple sclerosis—establishing disease prognosis and monitoring patients. *Nat Rev Neurol*. 2015;11:597-606.
3. Filippi M, Preziosa P, Banwell BL, et al. Assessment of lesions on magnetic resonance imaging in multiple sclerosis: Practical guidelines. *Brain*. 2019;142:1858-1875.
4. Pierpaoli C. Quantitative brain MRI. *Top Magn Reson Imaging*. 2010;21:63.
5. Lucchinetti C, Brück W, Parisi J, Scheithauer B, Rodriguez M, Lassmann H. Heterogeneity of multiple sclerosis lesions: Implications for the pathogenesis of demyelination. *Ann Neurol*. 2000;47:707-717.
6. van der Valk P, De Groot CJ. Staging of multiple sclerosis (MS) lesions: Pathology of the time frame of MS. *Neuropathol Appl Neurobiol*. 2000;26:2-10.
7. Barnett MH, Prineas JW. Relapsing and remitting multiple sclerosis: Pathology of the newly forming lesion. *Ann Neurol*. 2004;55:458-468.
8. Luchicchi AK, Perna L, Frigerio I, Hart BA, Stys PK, Schenk GJ, Geurts JJG. Disturbed axon-myelin interaction in MS normal appearing white matter. Stockholm, Sweden:ECTRIMS; 2019.
9. Dutta R, Chang A, Doud MK, et al. Demyelination causes synaptic alterations in hippocampi from multiple sclerosis patients. *Ann Neurol*. 2011;69:445-454.
10. Helms G. Tissue properties from quantitative MRI. In: AW Toga, ed. *Brain mapping: An encyclopedic reference*. Cambridge, MA: Academic Press; Elsevier; 2015. 287-294.
11. Stuber C, Morawski M, Schafer A, et al. Myelin and iron concentration in the human brain: A quantitative study of MRI contrast. *Neuroimage*. 2014;93:95-106.
12. Seewann A, Kooi EJ, Roosendaal SD, Barkhof F, van der Valk P, Geurts JJ. Translating pathology in multiple sclerosis: The combination of postmortem imaging, histopathology and clinical findings. *Acta Neurol Scand*. 2009;119:349-355.

13. Mottershead JP, Schmierer K, Clemence M, et al. High field MRI correlates of myelin content and axonal density in multiple sclerosis—a post-mortem study of the spinal cord. *J Neurol.* 2003;250:1293-1301.
14. Jonkman LE, Soriano AL, Amor S, et al. Can MS lesion stages be distinguished with MRI? A postmortem MRI and histopathology study. *J Neurol.* 2015;262:1074-1080.
15. Brex PA, Parker GJ, Leary SM, et al. Lesion heterogeneity in multiple sclerosis: A study of the relations between appearances on T1 weighted images, T1 relaxation times, and metabolite concentrations. *J Neurol Neurosurg Psychiatry.* 2000;68:627-632.
16. Kolb H. 7T MP2RAGE MRI for assessment of myelination status in white matter lesions of multiple sclerosis. Stockholm, Sweden: ECTRIMS; 2019.
17. Kober T, Granziera C, Ribes D, et al. MP2RAGE multiple sclerosis magnetic resonance imaging at 3 T. *Investigative Radiology.* 2012;47:346-352.
18. Schmierer K, Parkes HG, So PW, et al. High field (9.4 Tesla) magnetic resonance imaging of cortical grey matter lesions in multiple sclerosis. *Brain.* 2010;133:858-867.
19. Beck ES, Sati P, Sethi V, et al. Improved visualization of cortical lesions in multiple sclerosis using 7T MP2RAGE. *AJNR Am J Neuroradiol.* 2018;39:459-466.
20. Fartaria MJ, O'Brien K, Sorega A, et al. An ultra-high field study of cerebellar pathology in early relapsing-remitting multiple sclerosis using MP2RAGE. *Invest Radiol.* 2017;52:265-273.
21. Bonnier G, Fische-Gomez E, Roche A, et al. Personalized pathology maps to quantify diffuse and focal brain damage. *Neuroimage Clin.* 2019;21:101607.
22. Vrenken H, Geurts JJ, Knol DL, et al. Normal-appearing white matter changes vary with distance to lesions in multiple sclerosis. *AJNR Am J Neuroradiol.* 2006;27:2005-2011.
23. Vrenken H, Geurts JJ, Knol DL, et al. Whole-brain T1 mapping in multiple sclerosis: Global changes of normal-appearing gray and white matter. *Radiology.* 2006;240:811-820.
24. Thaler C, Faizy T, Sedlacik J, et al. T1-thresholds in black holes increase clinical-radiological correlation in multiple sclerosis patients. *PLoS One.* 2015;10:e0144693.
25. Thaler C, Faizy TD, Sedlacik J, et al. T1 recovery is predominantly found in black holes and is associated with clinical improvement in patients with multiple sclerosis. *AJNR Am J Neuroradiol.* 2017;38:264-269.
26. Simioni S, Amaru F, Bonnier G, et al. MP2RAGE provides new clinically-compatible correlates of mild cognitive deficits in relapsing-remitting multiple sclerosis. *J Neurol.* 2014;261:1606-1613.
27. Ropele S, Langkammer C, Enzinger C, Fuchs S, Fazekas F. Relaxation time mapping in multiple sclerosis. *Expert Rev Neurother.* 2011;11:441-450.
28. Taylor AJ, Salerno M, Dharmakumar R, Jerosch-Herold M. T1 mapping: Basic techniques and clinical applications. *JACC Cardiovasc Imaging.* 2016;9:67-81.
29. Stikov N, Boudreau M, Levesque IR, Tardif CL, Barral JK, Pike GB. On the accuracy of T1 mapping: Searching for common ground. *Magn Reson Med.* 2015;73:514-522.
30. Bane O, Hectors SJ, Wagner M, et al. Accuracy, repeatability, and interplatform reproducibility of T1 quantification methods used for DCE-MRI: Results from a multicenter phantom study. *Magn Reson Med.* 2018;79:2564-2575.
31. Marques JP, Kober T, Krueger G, van der Zwaag W, Van de Moortele PF, Gruetter R. MP2RAGE, a self bias-field corrected sequence for improved segmentation and T1-mapping at high field. *Neuroimage.* 2010;49:1271-1281.
32. Voelker MN, Kraff O, Brenner D, et al. The traveling heads: Multicenter brain imaging at 7 Tesla. *Magn Reson Mater Phys.* 2016;29:399-415.
33. Yen Y-FK, Stupic KF, van der Kouwe A, Polimeni JR. T1 mapping of NIST Phantom at 7T. Honolulu, HI, USA: International Society for Magnetic Resonance Imaging (ISMRM); 2017.
34. Warntjes JB, Leinhard OD, West J, Lundberg P. Rapid magnetic resonance quantification on the brain: Optimization for clinical usage. *Magn Reson Med.* 2008;60:320-329.
35. Hagiwara A, Warntjes M, Hori M, et al. SyMRI of the brain: Rapid quantification of relaxation rates and proton density, with synthetic MRI, automatic brain segmentation, and myelin measurement. *Invest Radiol.* 2017;52:647-657.
36. Hagiwara A, Hori M, Kamagata K, et al. Myelin measurement: Comparison between simultaneous tissue relaxometry, magnetization transfer saturation index, and T1w/T2w ratio. *Sci Rep.* 2018;8:10554.
37. Rasoanandrianina H, Massire A, Taso M, et al. Regional T1 mapping of the whole cervical spinal cord using an optimized MP2RAGE sequence. *NMR Biomed.* 2019;32:e4142.
38. Cortese R, Collorone S, Ciccarelli O, Toosy AT. Advances in brain imaging in multiple sclerosis. *Ther Adv Neurol Disord.* 2019;12:175628641985972.
39. O'Muircheartaigh J, Vavasour I, Ljungberg E, et al. Quantitative neuroimaging measures of myelin in the healthy brain and in multiple sclerosis. *Hum Brain Mapp.* 2019;40:2104-2116.
40. Agosta F, Rovaris M, Pagani E, Sormani MP, Comi G, Filippi M. Magnetization transfer MRI metrics predict the accumulation of disability 8 years later in patients with multiple sclerosis. *Brain.* 2006;129:2620-2627.
41. Rovaris M, Agosta F, Sormani MP, et al. Conventional and magnetization transfer MRI predictors of clinical multiple sclerosis evolution: A medium-term follow-up study. *Brain.* 2003;126:2323-2332.
42. Cadavid D, Mellion M, Hupperts R, et al. Safety and efficacy of opicinumab in patients with relapsing multiple sclerosis (SYNERGY): A randomised, placebo-controlled, phase 2 trial. *Lancet Neurol.* 2019;18:845-856.
43. Kremer D, Gottle P, Flores-Rivera J, Hartung HP, Kury P. Remyelination in multiple sclerosis: From concept to clinical trials. *Curr Opin Neurol.* 2019;32:378-384.
44. MacKay AL, Laule C. Magnetic resonance of myelin water: An in vivo marker for myelin. *Brain Plast.* 2016;2:71-91.
45. Whittall KP, MacKay AL, Li DK. Are mono-exponential fits to a few echoes sufficient to determine T2 relaxation for in vivo human brain? *Magn Reson Med.* 1999;41:1255-1257.
46. Laule C, Leung E, Li DK, et al. Myelin water imaging in multiple sclerosis: Quantitative correlations with histopathology. *Mult Scler.* 2006;12:747-753.
47. Bonnier G, Roche A, Romascano D, et al. Advanced MRI unravels the nature of tissue alterations in early multiple sclerosis. *Ann Clin Transl Neurol.* 2014;1:423-432.
48. Warntjes M, Engstrom M, Tisell A, Lundberg P. Modeling the presence of myelin and edema in the brain based on multi-parametric quantitative MRI. *Front Neurol.* 2016;7:16.
49. Bot JC, Blezer EL, Kamphorst W, et al. The spinal cord in multiple sclerosis: Relationship of high-spatial-resolution quantitative MR imaging findings to histopathologic results. *Radiology.* 2004;233:531-540.
50. Langkammer C, Krebs N, Goessler W, et al. Quantitative MR imaging of brain iron: A postmortem validation study. *Radiology.* 2010;257:455-462.
51. Laule C, Moore GRW. Myelin water imaging to detect demyelination and remyelination and its validation in pathology. *Brain Pathol.* 2018;28:750-764.
52. Birkel C, Birkel-Toeglhofer AM, Endmayr V, et al. The influence of brain iron on myelin water imaging. *Neuroimage.* 2019;199:545-552.doi: 10.1016/j.neuroimage.2019.05.042.
53. Schmierer K, Scaravilli F, Altmann DR, Barker GJ, Miller DH. Magnetization transfer ratio and myelin in postmortem multiple sclerosis brain. *Ann Neurol.* 2004;56:407-415.
54. van Waesberghe JH, Kamphorst W, De Groot CJ, et al. Axonal loss in multiple sclerosis lesions: Magnetic resonance imaging

- insights into substrates of disability. *Ann Neurol.* 1999;46:747-754.
55. Moccia M, van de Pavert S, Eshaghi A, et al. Pathological correlates of the magnetization transfer ratio in multiple sclerosis. *Neurology.* 2020;95:e2965-e2976.
  56. Ouellette R, Mangeat G, Polyak I, et al. Validation of rapid magnetic resonance myelin imaging in multiple sclerosis. *Ann Neurol.* 2020;87:710-724.
  57. Neema M, Goldberg-Zimring D, Guss ZD, et al. 3 T MRI relaxometry detects T2 prolongation in the cerebral normal-appearing white matter in multiple sclerosis. *Neuroimage.* 2009;46:633-641.
  58. Romascano D, Meskaldji DE, Bonnier G, et al. Multicontrast connectometry: a new tool to assess cerebellum alterations in early relapsing-remitting multiple sclerosis. *Hum Brain Mapp.* 2015;36:1609-1619.
  59. Whittall KP, MacKay AL, Li DK, Vavasour IM, Jones CK, Paty DW. Normal-appearing white matter in multiple sclerosis has heterogeneous, diffusely prolonged T(2). *Magn Reson Med.* 2002;47:403-408.
  60. Gracien RM, Reitz SC, Hof SM, et al. Assessment of cortical damage in early multiple sclerosis with quantitative T2 relaxometry. *NMR Biomed.* 2016;29:444-450.
  61. Chatterjee S, Commowick O, Afacan O, Warfield SK, Barillot C. Identification of Gadolinium contrast enhanced regions in MS lesions using brain tissue microstructure information obtained from diffusion and T2 relaxometry MRI. In: *21st International Conference on Medical Image Computing and Computer Assisted Intervention (MICCAI 2018)*. Grenade, Spain: Springer; 2018. 63-71.
  62. Vargas WS, Monohan E, Pandya S, et al. Measuring longitudinal myelin water fraction in new multiple sclerosis lesions. *Neuroimage Clin.* 2015;9:369-375.
  63. Yao Y, Nguyen TD, Pandya S, et al. Combining quantitative susceptibility mapping with automatic zero reference (QSM0) and myelin water fraction imaging to quantify iron-related myelin damage in chronic active MS lesions. *AJNR Am J Neuroradiol.* 2018;39:303-310.
  64. Kolind S, Seddigh A, Combes A, et al. Brain and cord myelin water imaging: A progressive multiple sclerosis biomarker. *Neuroimage Clin.* 2015;9:574-580.
  65. Laule C, Vavasour IM, Zhao Y, et al. Two-year study of cervical cord volume and myelin water in primary progressive multiple sclerosis. *Mult Scler.* 2010;16:670-677.
  66. Filippi M, Rocca MA, Martino G, Horsfield MA, Comi G. Magnetization transfer changes in the normal appearing white matter precede the appearance of enhancing lesions in patients with multiple sclerosis. *Ann Neurol.* 1998;43:809-814.
  67. Barkhof F, Bruck W, De Groot CJ, et al. Remyelinated lesions in multiple sclerosis: Magnetic resonance image appearance. *Arch Neurol.* 2003;60:1073-1081.
  68. Oh J, Ontaneda D, Azevedo C, et al. Imaging outcome measures of neuroprotection and repair in MS: A consensus statement from NAIMS. *Neurology.* 2019;92:519-533.
  69. van Waesberghe JH, van Walderveen MA, Castelijns JA, et al. Patterns of lesion development in multiple sclerosis: Longitudinal observations with T1-weighted spin-echo and magnetization transfer MR. *AJNR Am J Neuroradiol.* 1998;19:675-683.
  70. Chen JT, Collins DL, Atkins HL, Freedman MS, Arnold DL, Canadian M. Magnetization transfer ratio evolution with demyelination and remyelination in multiple sclerosis lesions. *Ann Neurol.* 2008;63:254-262.
  71. Combes B, Kerbrat A, Ferre JC, et al. Focal and diffuse cervical spinal cord damage in patients with early relapsing-remitting MS: A multicentre magnetisation transfer ratio study. *Mult Scler.* 2019;25:1113-1123.
  72. Kearney H, Rocca MA, Valsasina P, et al. Magnetic resonance imaging correlates of physical disability in relapse onset multiple sclerosis of long disease duration. *Mult Scler.* 2014;20:72-80.
  73. Samson RS, Cardoso MJ, Muhler N, et al. Investigation of outer cortical magnetisation transfer ratio abnormalities in multiple sclerosis clinical subgroups. *Mult Scler.* 2014;20:1322-1330.
  74. Oh J, Chen M, Cybulsky K, et al. Five-year longitudinal changes in quantitative spinal cord MRI in multiple sclerosis. *Mult Scler.* 2021;27:549-558.
  75. Lommers E, Simon J, Reuter G, et al. Multiparameter MRI quantification of microstructural tissue alterations in multiple sclerosis. *Neuroimage Clin.* 2019;23:101879.
  76. Saccenti L, Hagiwara A, Andica C, et al. Myelin measurement using quantitative magnetic resonance imaging: A correlation study comparing various imaging techniques in patients with multiple sclerosis. *Cells.* 2020;9:393.
  77. Bagnato F, Franco G, Ye F, et al. Selective inversion recovery quantitative magnetization transfer imaging: Toward a 3 T clinical application in multiple sclerosis. *Mult Scler.* 2020;26:457-467.
  78. Lema A, Bishop C, Malik O, et al. A comparison of magnetization transfer methods to assess brain and cervical cord microstructure in multiple sclerosis. *J Neuroimaging.* 2017;27:221-226.
  79. Dvorak AV, Wiggermann V, Gilbert G, et al. Multi-spin echo T2 relaxation imaging with compressed sensing (METRICS) for rapid myelin water imaging. *Magn Reson Med.* 2020;84:1264-1279.
  80. Hilbert T, Sumpf TJ, Weiland E, et al. Accelerated T2 mapping combining parallel MRI and model-based reconstruction: GRAPPATINI. *J Magn Reson Imaging.* 2018;48:359-368.
  81. Nguyen TD, Deh K, Monohan E, et al. Feasibility and reproducibility of whole brain myelin water mapping in 4 minutes using fast acquisition with spiral trajectory and adiabatic T2prep (FAST-T2) at 3T. *Magn Reson Med.* 2016;76:456-465.
  82. Piredda GF, Hilbert T, Canales-Rodriguez EJ, et al. Fast and high-resolution myelin water imaging: Accelerating multi-echo GRASE with CAIPIRINHA. *Magn Reson Med.* 2021;85:209-222.
  83. Dvorak AV, Ljungberg E, Vavasour IM, et al. Rapid myelin water imaging for the assessment of cervical spinal cord myelin damage. *Neuroimage Clin.* 2019;23:101896.
  84. Barker GJ, Schreiber WG, Gass A, et al. A standardised method for measuring magnetisation transfer ratio on MR imagers from different manufacturers-the EuroMT sequence. *Magma.* 2005;18:76-80.
  85. Ropele S, Filippi M, Valsasina P, et al. Assessment and correction of B1-induced errors in magnetization transfer ratio measurements. *Magn Reson Med.* 2005;53:134-140.
  86. Weiskopf N, Suckling J, Williams G, et al. Quantitative multiparameter mapping of R1, PD(), MT, and R2() at 3T: A multicenter validation. *Front Neurosci.* 2013;7:95.
  87. Meyers SM, Laule C, Vavasour IM, et al. Reproducibility of myelin water fraction analysis: A comparison of region of interest and voxel-based analysis methods. *Magn Reson Imaging.* 2009;27:1096-1103.
  88. Lee LE, Ljungberg E, Shin D, et al. Inter-vendor reproducibility of myelin water imaging using a 3D gradient and spin echo sequence. *Front Neurosci.* 2018;12:854.
  89. Levy S, Guertin MC, Khatibi A, et al. Test-retest reliability of myelin imaging in the human spinal cord: Measurement errors versus region- and aging-induced variations. *PLoS One.* 2018;13:e0189944.
  90. Basser PJ, Mattiello J, LeBihan D. MR diffusion tensor spectroscopy and imaging. *Biophys J.* 1994;66:259-267.
  91. Bodini B, Cercignani M, Toosy A, et al. A novel approach with "skeletonised MTR" measures tract-specific microstructural changes in early primary-progressive MS. *Hum Brain Mapp.* 2014;35:723-733.
  92. Pierpaoli C, Jezzard P, Basser PJ, Barnett A, Di Chiro G. Diffusion tensor MR imaging of the human brain. *Radiology.* 1996;201:637-648.
  93. Song SK, Sun SW, Ramsbottom MJ, Chang C, Russell J, Cross AH. Demyelination revealed through MRI as increased radial

- (but unchanged axial) diffusion of water. *Neuroimage*. 2002;17:1429-1436.
94. Novikov DS, Fieremans E, Jespersen SN, Kiselev VG. Quantifying brain microstructure with diffusion MRI: Theory and parameter estimation. *NMR Biomed*. 2019;32:e3998.
  95. Ferizi U, Scherrer B, Schneider T, et al. Diffusion MRI microstructure models with in vivo human brain Connectome data: Results from a multi-group comparison. *NMR Biomed*. 2017;30:e3734.
  96. Assaf Y, Freidlin RZ, Rohde GK, Basser PJ. New modeling and experimental framework to characterize hindered and restricted water diffusion in brain white matter. *Magn Reson Med*. 2004;52:965-978.
  97. Assaf Y, Blumenfeld-Katzir T, Yovel Y, Basser PJ. AxCaliber: A method for measuring axon diameter distribution from diffusion MRI. *Magn Reson Med*. 2008;59:1347-1354.
  98. Barazany D, Basser PJ, Assaf Y. In vivo measurement of axon diameter distribution in the corpus callosum of rat brain. *Brain*. 2009;132:1210-1220.
  99. Alexander DC, Hubbard PL, Hall MG, et al. Orientationally invariant indices of axon diameter and density from diffusion MRI. *Neuroimage*. 2010;52:1374-1389.
  100. Wu EX, Cheung MM. MR diffusion kurtosis imaging for neural tissue characterization. *NMR Biomed*. 2010;23:836-848.
  101. Chiang CW, Wang Y, Sun P, et al. Quantifying white matter tract diffusion parameters in the presence of increased extra-fiber cellularity and vasogenic edema. *Neuroimage*. 2014;101:310-319.
  102. Cross AH, Song SK. A new imaging modality to non-invasively assess multiple sclerosis pathology. *J Neuroimmunol*. 2017;304:81-85.
  103. Zhang H, Schneider T, Wheeler-Kingshott CA, Alexander DC. NODDI: Practical in vivo neurite orientation dispersion and density imaging of the human brain. *Neuroimage*. 2012;61:1000-1016.
  104. Palombo M, Ianus A, Guerreri M, et al. SANDI: A compartment-based model for non-invasive apparent soma and neurite imaging by diffusion MRI. *Neuroimage*. 2020;215:116835.
  105. Özarlan E, Koay CG, Shepherd TM, et al. Mean apparent propagator (MAP) MRI: A novel diffusion imaging method for mapping tissue microstructure. *Neuroimage*. 2013;78:16-32.
  106. Descoteaux M, Deriche R, Le Bihan D, Mangin JF, Poupon C. Multiple q-shell diffusion propagator imaging. *Med Image Anal*. 2011;15:603-621.
  107. Hosseinbor AP, Chung MK, Wu YC, Alexander AL. Bessel Fourier Orientation Reconstruction (BFOR): An analytical diffusion propagator reconstruction for hybrid diffusion imaging and computation of q-space indices. *Neuroimage*. 2013;64:650-670.
  108. Schmierer K, Wheeler-Kingshott CA, Boulby PA, et al. Diffusion tensor imaging of post mortem multiple sclerosis brain. *Neuroimage*. 2007;35:467-477.
  109. Preziosa P, Kiljan S, Steenwijk MD, et al. Axonal degeneration as substrate of fractional anisotropy abnormalities in multiple sclerosis cortex. *Brain*. 2019;142:1921-1937.
  110. Cercignani M, Gandini Wheeler-Kingshott C. From micro- to macro-structures in multiple sclerosis: What is the added value of diffusion imaging. *NMR Biomed*. 2019;32:e3888.
  111. Klawiter EC, Schmidt RE, Trinkaus K, et al. Radial diffusivity predicts demyelination in ex vivo multiple sclerosis spinal cords. *Neuroimage*. 2011;55:1454-1460.
  112. Wheeler-Kingshott CA, Cercignani M. About "axial" and "radial" diffusivities. *Magn Reson Med*. 2009;61:1255-1260.
  113. Wheeler-Kingshott CA, Ciccarelli O, Schneider T, Alexander DC, Cercignani M. A new approach to structural integrity assessment based on axial and radial diffusivities. *Funct Neurol*. 2012;27:85-90.
  114. Grussu F, Schneider T, Tur C, et al. Neurite dispersion: A new marker of multiple sclerosis spinal cord pathology? *Ann Clin Transl Neurol*. 2017;4:663-679.
  115. Mollink J, Kleinnijenhuis M, Cappellen van Walsum AV, et al. Evaluating fibre orientation dispersion in white matter: Comparison of diffusion MRI, histology and polarized light imaging. *Neuroimage*. 2017;157:561-574.
  116. Shirani A, Sun P, Schmidt RE, et al. Histopathological correlation of diffusion basis spectrum imaging metrics of a biopsy-proven inflammatory demyelinating brain lesion: A brief report. *Mult Scler*. 2019;25:1937-1941.
  117. Rocca MA, Cercignani M, Iannucci G, Comi G, Filippi M. Weekly diffusion-weighted imaging of normal-appearing white matter in MS. *Neurology*. 2000;55:882-884.
  118. Werring DJ, Brassat D, Droogan AG, et al. The pathogenesis of lesions and normal-appearing white matter changes in multiple sclerosis: A serial diffusion MRI study. *Brain*. 2000;123:1667-1676.
  119. Wang KY, Carlton J, Guffey D, Hutton GJ, Moron FE. Histogram analysis of apparent diffusion coefficient and fluid-attenuated inversion recovery in discriminating between enhancing and nonenhancing lesions in multiple sclerosis. *Clin Imaging*. 2020;59:13-20.
  120. Naismith RT, Xu J, Tutlam NT, et al. Increased diffusivity in acute multiple sclerosis lesions predicts risk of black hole. *Neurology*. 2010;74:1694-1701.
  121. Harel A, Sperling D, Petracca M, et al. Brain microstructural injury occurs in patients with RRMS despite 'no evidence of disease activity'. *J Neurol Neurosurg Psychiatry*. 2018;89:977-982.
  122. Vinciguerra C, Giorgio A, Zhang J, et al. Peak width of skeletonized mean diffusivity (PSMD) as marker of widespread white matter tissue damage in multiple sclerosis. *Mult Scler Relat Disord*. 2019;27:294-297.
  123. Kearney H, Schneider T, Yiannakas MC, et al. Spinal cord grey matter abnormalities are associated with secondary progression and physical disability in multiple sclerosis. *J Neurol Neurosurg Psychiatry*. 2015;86:608-614.
  124. Toosy AT, Kou N, Altmann D, Wheeler-Kingshott CA, Thompson AJ, Ciccarelli O. Voxel-based cervical spinal cord mapping of diffusion abnormalities in MS-related myelitis. *Neurology*. 2014;83:1321-1325.
  125. Kolasa M, Hakulinen U, Brander A, et al. Diffusion tensor imaging and disability progression in multiple sclerosis: A 4-year follow-up study. *Brain Behav*. 2019;9:e011194.
  126. Eijlers AJC, van Geest Q, Dekker I, et al. Predicting cognitive decline in multiple sclerosis: A 5-year follow-up study. *Brain*. 2018;141:2605-2618.
  127. Rocca MA, Sormani MP, Rovaris M, et al. Long-term disability progression in primary progressive multiple sclerosis: A 15-year study. *Brain*. 2017;140:2814-2819.
  128. Naismith RT, Xu J, Tutlam NT, Trinkaus K, Cross AH, Song SK. Radial diffusivity in remote optic neuritis discriminates visual outcomes. *Neurology*. 2010;74:1702-1710.
  129. Naismith RT, Xu J, Klawiter EC, et al. Spinal cord tract diffusion tensor imaging reveals disability substrate in demyelinating disease. *Neurology*. 2013;80:2201-2209.
  130. Freund P, Wheeler-Kingshott C, Jackson J, Miller D, Thompson A, Ciccarelli O. Recovery after spinal cord relapse in multiple sclerosis is predicted by radial diffusivity. *Mult Scler*. 2010;16:1193-1202.
  131. Agosta F, Absinta M, Sormani MP, et al. In vivo assessment of cervical cord damage in MS patients: A longitudinal diffusion tensor MRI study. *Brain*. 2007;130:2211-2219.
  132. Guglielmetti C, Veraart J, Roelant E, et al. Diffusion kurtosis imaging probes cortical alterations and white matter pathology following cuprizone induced demyelination and spontaneous remyelination. *Neuroimage*. 2016;125:363-377.
  133. de Kouchkovsky I, Fieremans E, Fleysher L, Herbert J, Grossman RI, Inglese M. Quantification of normal-appearing white matter tract integrity in multiple sclerosis: A diffusion kurtosis imaging study. *J Neurol*. 2016;263:1146-1155.

134. Shirani A, Sun P, Trinkaus K, et al. Diffusion basis spectrum imaging for identifying pathologies in MS subtypes. *Ann Clin Transl Neurol.* 2019;6:2323-2327.
135. Sun P, George A, Perantie DC, et al. Diffusion basis spectrum imaging provides insights into MS pathology. *Neurol Neuroimmunol Neuroinflamm.* 2020;7:e655.
136. De Santis S, Granberg T, Ouellette R, et al. Early axonal damage in normal appearing white matter in multiple sclerosis: Novel insights from multi-shell diffusion MRI. *Conf Proc IEEE Eng Med Biol Soc.* 2017;2017:3024-3027.
137. Toschi N, De Santis S, Granberg T, et al. Evidence for progressive microstructural damage in early multiple sclerosis by multi-shell diffusion magnetic resonance imaging. *Neuroscience.* 2019;403:27-34.
138. Granberg T, Fan Q, Treaba CA, et al. In vivo characterization of cortical and white matter neuroaxonal pathology in early multiple sclerosis. *Brain.* 2017;140:2912-2926.
139. Spano B, Giulietti G, Pisani V, et al. Disruption of neurite morphology parallels MS progression. *Neurol Neuroimmunol Neuroinflamm.* 2018;5:e502.
140. By S, Xu J, Box BA, Bagnato FR, Smith SA. Application and evaluation of NODDI in the cervical spinal cord of multiple sclerosis patients. *Neuroimage Clin.* 2017;15:333-342.
141. Collorone S, Cawley N, Grussu F, et al. Reduced neurite density in the brain and cervical spinal cord in relapsing-remitting multiple sclerosis: A NODDI study. *Mult Scler.* 2020;26:1647-1657.
142. Abdel-Aziz K, Schneider T, Solanky BS, et al. Evidence for early neurodegeneration in the cervical cord of patients with primary progressive multiple sclerosis. *Brain.* 2015;138:1568-1582.
143. Cortese R, Tur C, Prados F, et al. Ongoing microstructural changes in the cervical cord underpin disability progression in early primary progressive multiple sclerosis. *Mult Scler.* 2021;27:28-38.
144. Acheson A, Wijtenburg SA, Rowland LM, et al. Reproducibility of tract-based white matter microstructural measures using the ENIGMA-DTI protocol. *Brain Behav.* 2017;7:e00615.
145. Grech-Sollars M, Hales PW, Miyazaki K, et al. Multi-centre reproducibility of diffusion MRI parameters for clinical sequences in the brain. *NMR Biomed.* 2015;28:468-485.
146. Heiervang E, Behrens TE, Mackay CE, Robson MD, Johansen-Berg H. Between session reproducibility and between subject variability of diffusion MR and tractography measures. *Neuroimage.* 2006;33:867-877.
147. Magnotta VA, Matsui JT, Liu D, et al. Multicenter reliability of diffusion tensor imaging. *Brain Connect.* 2012;2:345-355.
148. Nencka AS, Meier TB, Wang Y, et al. Stability of MRI metrics in the advanced research core of the NCAA-DoD concussion assessment, research and education (CARE) consortium. *Brain Imaging Behav.* 2018;12:1121-1140.
149. Prohl AK, Scherrer B, Tomas-Fernandez X, et al. Reproducibility of structural and diffusion tensor imaging in the TACERN multicenter study. *Front Integr Neurosci.* 2019;13:24.
150. Zhou X, Sakaie KE, Debbins JP, Narayanan S, Fox RJ, Lowe MJ. Scan-rescan repeatability and cross-scanner comparability of DTI metrics in healthy subjects in the SPRINT-MS multicenter trial. *Magn Reson Imaging.* 2018;53:105-111.
151. Andica C, Kamagata K, Hayashi T, et al. Scan-rescan and inter-vendor reproducibility of neurite orientation dispersion and density imaging metrics. *Neuroradiology.* 2020;62:483-494.
152. Chung AW, Seunarine KK, Clark CA. NODDI reproducibility and variability with magnetic field strength: A comparison between 1.5 T and 3 T. *Hum Brain Mapp.* 2016;37:4550-4565.
153. Samson RS, Levy S, Schneider T, et al. ZOOM or Non-ZOOM? Assessing spinal cord diffusion tensor imaging protocols for multi-centre studies. *PLoS One.* 2016;11:e0155557.
154. Langkammer C, Liu T, Khalil M, et al. Quantitative susceptibility mapping in multiple sclerosis. *Radiology.* 2013;267:551-559.
155. Duyn JH, Schenck J. Contributions to magnetic susceptibility of brain tissue. *NMR Biomed.* 2017;30: 10.1002/nbm.3546.
156. Denk C, Hernandez Torres E, MacKay A, Rauscher A. The influence of white matter fibre orientation on MR signal phase and decay. *NMR Biomed.* 2011;24:246-252.
157. He X, Yablonskiy DA. Biophysical mechanisms of phase contrast in gradient echo MRI. *Proc Natl Acad Sci U S A.* 2009;106:13558-13563.
158. Lancione M, Tosetti M, Donatelli G, Cosottini M, Costagli M. The impact of white matter fiber orientation in single-acquisition quantitative susceptibility mapping. *NMR Biomed.* 2017;30: 10.1002/nbm.3798.
159. Wiggermann V, Hametner S, Hernandez-Torres E, et al. Susceptibility-sensitive MRI of multiple sclerosis lesions and the impact of normal-appearing white matter changes. *NMR Biomed.* 2017;30: 10.1002/nbm.3727.
160. Hernandez-Torres E, Wiggermann V, Hametner S, et al. Orientation dependent MR signal decay differentiates between people with MS, their asymptomatic siblings and unrelated healthy controls. *PLoS One.* 2015;10:e0140956.
161. Dong J, Liu T, Chen F, et al. Simultaneous phase unwrapping and removal of chemical shift (SPURS) using graph cuts: Application in quantitative susceptibility mapping. *IEEE Trans Med Imaging.* 2015;34:531-540.
162. Li W, Liu C, Duong TQ, van Zijl PC, Li X. Susceptibility tensor imaging (STI) of the brain. *NMR Biomed.* 2017;30: 10.1002/nbm.3540.
163. Hametner S, Endmayer V, Deistung A, et al. The influence of brain iron and myelin on magnetic susceptibility and effective transverse relaxation - A biochemical and histological validation study. *Neuroimage.* 2018;179:117-133.
164. Dal-Bianco A, Grabner G, Kronnerwetter C, et al. Slow expansion of multiple sclerosis iron rim lesions: Pathology and 7 T magnetic resonance imaging. *Acta Neuropathol.* 2017;133:25-42.
165. Wisnieff C, Ramanan S, Olesik J, Gauthier S, Wang Y, Pitt D. Quantitative susceptibility mapping (QSM) of white matter multiple sclerosis lesions: Interpreting positive susceptibility and the presence of iron. *Magn Reson Med.* 2015;74:564-570.
166. Deh K, Ponath GD, Molvi Z, et al. Magnetic susceptibility increases as diamagnetic molecules breakdown: Myelin digestion during multiple sclerosis lesion formation contributes to increase on QSM. *J Magn Reson Imaging.* 2018;48:1281-1287.
167. Zhang Y, Gauthier SA, Gupta A, et al. Magnetic susceptibility from quantitative susceptibility mapping can differentiate new enhancing from nonenhancing multiple sclerosis lesions without gadolinium injection. *AJNR Am J Neuroradiol.* 2016;37:1794-1799.
168. Absinta M, Sati P, Masuzzo F, et al. Association of chronic active multiple sclerosis lesions with disability in vivo. *JAMA Neurol.* 2019;76:1474.
169. Schmalbrock P, Prakash RS, Schirda B, et al. Basal ganglia iron in patients with multiple sclerosis measured with 7T quantitative susceptibility mapping correlates with inhibitory control. *AJNR Am J Neuroradiol.* 2016;37:439-446.
170. Fan AP, Govindarajan ST, Kinkel RP, et al. Quantitative oxygen extraction fraction from 7-Tesla MRI phase: Reproducibility and application in multiple sclerosis. *J Cereb Blood Flow Metab.* 2015;35:131-139.
171. Langkammer C, Schweser F, Shmueli K, et al. Quantitative susceptibility mapping: Report from the 2016 reconstruction challenge. *Magn Reson Med.* 2018;79:1661-1673.
172. Deh K, Nguyen TD, Eskreis-Winkler S, et al. Reproducibility of quantitative susceptibility mapping in the brain at two field strengths from two vendors. *J Magn Reson Imaging.* 2015;42:1592-1600.
173. Deh K, Kawaji K, Bulk M, et al. Multicenter reproducibility of quantitative susceptibility mapping in a gadolinium phantom using MEDI+0 automatic zero referencing. *Magn Reson Med.* 2019;81:1229-1236.
174. D'Haeseleer M, Hostenbach S, Peeters I, et al. Cerebral hypoperfusion: A new pathophysiologic concept in multiple sclerosis? *J Cereb Blood Flow Metab.* 2015;35:1406-1410.



175. D'Haeseleer M, Beelen R, Fierens Y, et al. Cerebral hypoperfusion in multiple sclerosis is reversible and mediated by endothelin-1. *Proc Natl Acad Sci U S A*. 2013;110:5654-5658.
176. Wuerfel J, Bellmann-Strobl J, Brunecker P, et al. Changes in cerebral perfusion precede plaque formation in multiple sclerosis: A longitudinal perfusion MRI study. *Brain*. 2004;127:111-119.
177. Holland CM, Charil A, Csapo I, et al. The relationship between normal cerebral perfusion patterns and white matter lesion distribution in 1,249 patients with multiple sclerosis. *J Neuroimaging*. 2012;22:129-136.
178. Amann M, Achtnichts L, Hirsch JG, et al. 3D GRASE arterial spin labelling reveals an inverse correlation of cortical perfusion with the white matter lesion volume in MS. *Mult Scler*. 2012;18:1570-1576.
179. Bester M, Forkert ND, Stellmann JP, et al. Increased perfusion in normal appearing white matter in high inflammatory multiple sclerosis patients. *PLoS One*. 2015;10:e0119356.
180. Inglese M, Adhya S, Johnson G, et al. Perfusion magnetic resonance imaging correlates of neuropsychological impairment in multiple sclerosis. *J Cereb Blood Flow Metab*. 2008;28:164-171.
181. Adhya S, Johnson G, Herbert J, et al. Pattern of hemodynamic impairment in multiple sclerosis: Dynamic susceptibility contrast perfusion MR imaging at 3.0 T. *Neuroimage*. 2006;33:1029-1035.
182. Inglese M, Park SJ, Johnson G, et al. Deep gray matter perfusion in multiple sclerosis: Dynamic susceptibility contrast perfusion magnetic resonance imaging at 3 T. *Arch Neurol*. 2007;64:196-202.
183. Debernard L, Melzer TR, Van Stockum S, et al. Reduced grey matter perfusion without volume loss in early relapsing-remitting multiple sclerosis. *J Neurol Neurosurg Psychiatry*. 2014;85:544-551.
184. Lagana MM, Pelizzari L, Baglio F. Relationship between MRI perfusion and clinical severity in multiple sclerosis. *Neural Regen Res*. 2020;15:646-652.
185. Garaci FG, Marziali S, Meschini A, et al. Brain hemodynamic changes associated with chronic cerebrospinal venous insufficiency are not specific to multiple sclerosis and do not increase its severity. *Radiology*. 2012;265:233-239.
186. Paling D, Thade Petersen E, Tozer DJ, et al. Cerebral arterial bolus arrival time is prolonged in multiple sclerosis and associated with disability. *J Cereb Blood Flow Metab*. 2014;34:34-42.
187. Sowa P, Nygaard GO, Bjornerud A, Celius EG, Harbo HF, Beyer MK. Magnetic resonance imaging perfusion is associated with disease severity and activity in multiple sclerosis. *Neuroradiology*. 2017;59:655-64.
188. Aviv RI, Francis PL, Tenenbein R, et al. Decreased frontal lobe gray matter perfusion in cognitively impaired patients with secondary-progressive multiple sclerosis detected by the bookend technique. *AJNR Am J Neuroradiol*. 2012;33:1779-1785.
189. Francis PL, Jakubovic R, O'Connor P, et al. Robust perfusion deficits in cognitively impaired patients with secondary-progressive multiple sclerosis. *AJNR Am J Neuroradiol*. 2013;34:62-67.
190. Hojjat SP, Kincal M, Vitorino R, et al. Cortical perfusion alteration in normal-appearing gray matter is most sensitive to disease progression in relapsing-remitting multiple sclerosis. *AJNR Am J Neuroradiol*. 2016;37:1454-1461.
191. Vitorino R, Hojjat SP, Cantrell CG, et al. Regional frontal perfusion deficits in relapsing-remitting multiple sclerosis with cognitive decline. *AJNR Am J Neuroradiol*. 2016;37:1800-1807.
192. Jakimovski D, Topolski M, Genovese AV, Weinstock-Guttman B, Zivadinov R. Vascular aspects of multiple sclerosis: Emphasis on perfusion and cardiovascular comorbidities. *Expert Rev Neurother*. 2019;19:445-458.
193. Marshall O, Lu H, Brisset JC, et al. Impaired cerebrovascular reactivity in multiple sclerosis. *JAMA Neurol*. 2014;71:1275-1281.
194. Almeida JRC, Greenberg T, Lu H, et al. Test-retest reliability of cerebral blood flow in healthy individuals using arterial spin labeling: Findings from the EMBARC study. *Magn Reson Imaging*. 2018;45:26-33.
195. Artzi M, Liberman G, Blumenthal DT, Bokstein F, Aizenstein O, Ben Bashat D. Repeatability of dynamic contrast enhanced vp parameter in healthy subjects and patients with brain tumors. *J Neurooncol*. 2018;140:727-737.
196. Gevers S, van Osch MJ, Bokkers RP, et al. Intra- and multicenter reproducibility of pulsed, continuous and pseudo-continuous arterial spin labeling methods for measuring cerebral perfusion. *J Cereb Blood Flow Metab*. 2011;31:1706-1715.
197. Liu H, Ljungberg E, Dvorak AV, et al. Myelin water fraction and intra/extracellular water geometric mean T2 normative atlases for the cervical spinal cord from 3T MRI. *J Neuroimaging*. 2020;30:50-57.
198. Liu H, Rubino C, Dvorak AV, et al. Myelin water atlas: A template for myelin distribution in the brain. *J Neuroimaging*. 2019;29:699-706.
199. Piredda GF, Hilbert T, Granziera C, et al. Quantitative brain relaxation atlases for personalized detection and characterization of brain pathology. *Magn Reson Med*. 2020;83:337-351.